Republic of Iraq
Ministry of Higher Education
And Scientific Research
University Of Misan
College of Science

Preparation , Characterization of Biological Hydroxyapatite from Natural Sources for Some Biomedical Applications

A Thesis Submitted to
the College of Science / University of Misan As Partial Fulfillment
of the Requirements for the Master Degree of Science in Chemistry

By

Doaa Abbood Challoob Al - Mossawy

B.Sc. Chemistry / Misan University (2014)

Supervisor

Asst. Prof. Dr. Ali Taha Saleh

"Supervisor Certification"

I certify that this which entitled:

(Preparation, Characterization of Biological Hydroxyapatite From Natural Sources for Some Biomedical Applications).

Presented by (**Doaa Abbood Challoob**) was prepared under me supervision in the Department of Chemistry, College of Science, University of Misan, as a partial fulfillment of the requirements for the Degree of Master in Chemistry.

Signature: .....

Asst. prof. Dr. Ali Taha Saleh
Chemistry department
Collage of Science / Misan university
Date: / / 2023

Head of Chemistry department recommendation
According to the recommendation of Supervisor, this thesis is forwarded to the examination committee for Approval.

Signature: .....

Asst. prof. Dr. Tahssen Saddam Fan. di
Head of Chemistry department
Collage of Science / Misan university
Date: / / 2023

" Examining Committee Certificate "

We the Examining Committee members, certify that we have read this thesis
entitled (**Preparation, Characterization of Biological Hydroxyapatite from Natural Sources for Some Biomedical Applications**) and examined
the student by (**Doaa Abbood Challoob**) in its contents and in our opinion it meets the standard of a thesis for the degree of master in chemistry with (Excellent) estimation.

Signature: .....
Professor
Dr. Faris Abdulridha Jassim
Chemistry department
Collage of Science / Basrah university
Date: / / 2023
(Chairman)

Signature: .....
Assistant Professor
Dr. Rashid Rahim Hateet
Biology department
Collage of Science / Misan university
Date: / / 2023
(Member)

Signature: .....
Assistant Professor
Dr. Jassim Abbas Hussain
Chemistry department
Collage of Science / Misan university
Date: / / 2023
(Member)

Signature: .....
Assistant Professor
Dr. Ali Taha Saleh
Chemistry department
Collage of Science / Misan university
Date: / / 2023
(Member and Supervisor)

I confirm the above approval decision of the Examination Committee

Signature: .....
Professor
Dr. Sabeeh Jassim Gattea
Date 21 / 6 / 2023
(Dean of Science Collage)

بِسْمِ اللّٰهِ الّرَحْمن الّرَحْيمِ

((يَرْفَعُ اللّٰهُ الّذِينَ آمَنْوا مِنْكُمْ والّذِينَ أُوْتُوا الّعِلْمَ دَرَجّاتٍ وَاللّٰهُ بِمْآ تَعّلَمُونَ خَبِير))

صَدَقَ اللّٰهُ الّعَلِيُ الّعَظْيم

" سورةالمجادلة .... الآية (11) "

Dedication

To Whom I can never forget , the one whose passing away made me sad , and my constant grief …..

My father "my God have mercy on him"

To The source of tenderness in my life , who illuminates the shadows of difficulties with her prayers …..

My mother

To The Happiness Buds , The Hope of my life M. Baqer , and Rawan ….

My Children

To Those how have supported me and waiting for my Success ….

My Brothers & My close Friends

To The one who has given me his knowlede ….

My supervisor

Doaa

Acknowledgements

Praise be God And thanks be to Him as it should be for the majesty of His countenance , the greatness of His authority , the number of His creation , the contentment of Himself , the weight of His Throne , and the supply of His words , who gave me health , strength , and facilitated the ways for me to accomplish this work , and the prayer and peace of Allah be upon our Master and prophet Muhammad and his divine good family .

I would like to express my sincere gratitude to my supervisors ,**Asst. Prof. Dr. Ali Taha saleh** for highly inspiring guidance , patience , motivation , enthusiasm and immense knowledge , continuous support for completing this thesis .

Also I express my sincere thanks and gratitude to my family for their help mein providing the appropriate ambiences for study .

Finally , I'd like to thank my post graduate classmates, best friends , my another family for supported me and stand with me , apology to all whom I have not mentioned with my respect . thanks for all .

Researcher

Contents

List of Figures

List of Tablets

List of Abbreviations

Abbreviations	Key
HAP	Hydroxyapatite
TCP	Tricalcium Phosphate
CaP	Calcium Phosphate
CPC	Calcium Phosphate
CDHA	Calcium-deficient
CS	Compression Strength
βTCP	β- Tricalcium Phosphate
SBF	Simulated body fluid
P	Pseudomonas aeruginosa aeruginosa
E. coli	Escherichia coli
BG	Bioactive Glasses
BCP	Biphasic Calcium Phosphate
MW	Microwave
MCPM	Monocalcium phosphate monohydrate
MCPH	Monocalcium phosphate monohydrate
MCPA	Monocalcium phosphate anhydrous
MCP	Monocalcium phosphate anhydrous
DCPD	Dicalcium phosphate dihydrate (Brushite)
DCPA	Dicalcium phosphate anhydrous (Monetite)
OCP	Octacalcium Phosphate
αTCP	α-Tricalcium Phosphate

Abbreviations	Key
TTCP	Tetracalcium Phosphate
ACP	Amorphous calcium phosphate
FWHM	Full width at half maximum
DDW	Doubled distilled water
FTIR	Fourier Transform Infrared Spectroscopy
XRD	X-Ray diffraction
EDX	Energy-dispersive X-ray spectroscopy
FESEM	Field Emission Scanning Electron Microscope
TEM	Transmission electron microscopy
UV	Ultraviolet Light
ICP-MS	Inductively coupled plasma mass spectrometry
LB	Luria-Bertani
SD	Standard deviation

List of Symbols

Symbols	Key
e.g	For Example
etc	Et Cetera
3D	Three-Dimensional
mol%	Percentage of Number of Moles
Ca/P	Calcium to Phosphate Ratio
wt%	Weight-Weight Percentage
Ppm	Part Per million
µm	Micrometer
i.e.	In other words
Å	Angstrom
°C	Temperature
Nm	Nanometre
2θ	2 Theta
mM	Millimole
M	Molarity
min	Minutes
H	Hours
eV	Electron Volt
mg/L	Milligram Per Liter
Xc	Degree of Crystallinity
m2/g	Square Meter per Gram

ABSTRACT

Hydroxyapatite (HAp) are often preferred over the other calcium phosphate-based biomaterials in orthopedic surgeries due to its ability to be resorbed under physiological conditions. Hydroxyapatite (HAp) is a biomaterial that can be extracted from natural wastes. HAp has been widely used in biomedical applications owing to its excellent bioactivity, high biocompatibility, and excellent osteoconduction. The thesis consists of three chapters, the first chapter is a general introduction about extraction of biological hydroxyapatite from natural sources for biomedical application. The second chapter describes the experimental which includes, preparation of samples and extraction of hydroxyapatite, the final chapter explains the results and discussion. In this study an array of novel extracted Hydroxyapatite (HAp) from Misan city,Iraq as the natural sources of bones, it consists fish bones, chicken and sheep bones by using calcination method in different temperature. The characterization done by X-Ray Diffraction (XRD), Field Emission Scanning Electron Microscopy (FESEM) attached with Energy Dispersive X-Ray Analysis (EDX), X-Ray and Fourier transform infrared spectroscoppe (FTIR) techniques were employed to evaluate the phase composition, surface morphology and chemical compositions of hydroxyapatite (HAp). The in vitro dissolution behaviour of all hydroxyapatite was evaluated by immersing the samples in the Simulated Body Fluid (SBF) over 14 days at 37 °C. Enhanced hydroxyapatite (HAp) coupled with good antimicrobial properties against *Escherichia coli (E. coli*, ATCC 25922 strains) and *Staphylococcus aureus*.) and suggest that hydroxyapatite (HAp) can be developed further into antibacterial bone. Release profiles of antibiotics suggest that the doped hydroxyapatite can also serve as controlled drug release systems, amoxicillin, tetracycline and cephalexin were incorporated into the hydroxyapatite and their release profiles showed a sustained drug release over 7 days loaded Hap from fish bone. Cumulative release of 75%, 79% and 95% were observed for, amoxicillin, tetracycline and cephalexin respectively. Whereas from chickens 75%, 86% and 96.3 respectively. With HAp from sheep bone 68%, 78% and 75.4 respectively.

CHAPTER ONE

INTRODUCTION

1.1 Overview

Waste materials from natural sources are important resources for extraction and recovery of valuable compounds. Transformation of these waste materials into valuable materials requires specific techniques and approaches. Hydroxyapatite (HAp) is a biomaterial that can be extracted from natural wastes. HAp has been widely used in biomedical applications owing to its excellent bioactivity, high biocompatibility, and excellent osteoconduction characteristics. Thus, HAp is gaining prominence for applications as orthopaedic implants and dental materials. The recent methods for extraction of HAp from natural sources including mammalian, aquatic or marine sources, shell sources, plants and algae, and from mineral sources. The extraction methods used to obtain hydroxyapatite are also described. The effect of extraction process and natural waste source on the critical properties of the HAp such as Ca/P ratio, crystallinity and phase assemblage, particle sizes, and morphology are discussed herein.

1.2 Human Bone

Bone is mainly composed of nonstoichiometric calcium phosphates (CaP) blended with trace number of different ions. Bone is a highly organized polymer/ceramic nanocomposite that gives shape to the skeleton of the body (1). It not only structurally supports the body but also acts as a good reservoir for different minerals like calcium and phosphate (2). Bone is dynamic in nature and has a special ability to regenerate or self-organize to a certain extent till the end of life.

Bones can be classified in two types 1: cortical bone also known as compact bone and 2: trabecular bone, known as cancellous or spongy bone. These two types are classified on the basis of their porosity and unit microstructure (3). Cortical bone is primarily present in the shaft of long bones. It is a dense structure with 5 to 10 % porosity. which is present as the outer shell around the cancellous bone at the end of joints (4). There are different types of cortical bones that can be differentiated on the basis of their microstructure. In contrast to the trabecular bone, cancellous bone is a highly porous structure with 50 to 90 % porosity It is present in the end of long bones, in the vertebrae and flat bones(5).

1.2 Main inorganic components of bones.

Various types of HA with different properties, that can be used for specific applications, may be synthesized from numerous sources. Depending on the crystal phase, e.g., CaP ceramics can be classified as hydroxyapatite [($Ca_{10}(PO_4)_6(OH_2)$)Ca/P=1.67 precipitatedhydroxyapatite[$Ca_{10-x}(HPO_4)_x(PO4)_{6-x}(OH)_{2-x}$,x=1.50,1.67,pHA]calciumdeficient hydroxyapatite [$Ca_{10-x}(HPO_4)_x(PO_4)_{6-x}(OH)_{2-x}$, x=1.50–1.67, CDHA] α-tricalcium phosphate [(α-$Ca_3(PO_4)_2$), Ca/P=1.50, α-TCP]; β-tricalcium phosphate [(β-$Ca_3(PO_4)_2$), Ca/P=1.50, β-TCP]; amorphous calcium phosphate (ACP, Ca/P= 1.25–1.55); biphasic calcium phosphate [$Ca_3(PO4)^{2+}$ $Ca10(PO4)_6(OH_2)$, Ca/P=1.50–1.67, BCP]; dicalcium phosphate anhydrous, monetite ($CaHPO_4$, Ca/P=1.00, DCPA); dicalcium phosphate dihydrous, brushite ($CaHPO_4.{}_2H_2O$, Ca/P=1.00, DCPD); carbonated apatite [$Ca_5(PO_5,CO_3)_2$, Ca/P=1.67, CA]; monocalcium phosphate monohydrate [Ca $(H_2PO_4)_2 \cdot H_2O$, Ca/P=0.50, MCPM]; octacalcium phosphate [Ca_8 $H_2(PO_4)_6.5H_2O$, Ca/P= 1.33, OCP] and tetracalcium phosphate [CaO. Ca $(PO_4)_2$, Ca/P= 2.0, TTPC]. Among these various CaP ceramics HA and its combination with TCP are widely used as bone substitute materials and coatings on dental implants owing to their close chemical and crystallographic structure similarity to the inorganic components of bones (Fig. 1) and teeth.(6-11) Furthermore, CaP ceramics are indispensable hard tissue reconstruction materials due to their excellent bioactivity, biocompatibility, non-toxicity, non-immunogenicity and non-inflammatory behavior (6, 12).

1.4 Biomaterials

Biomaterials have been gaining increasing importance owing to their applicability to ageing populations and treatment of diseases. Research on developing new biomaterials or manipulating the structure and composition of existing biomaterials has been intensively focussed in order to enhance the properties of biomedical devices(13). In general, biomaterials are commonly used as implants, tissues, and organ transplants and in drug delivery systems (6). The biomaterials act to restore, repair, or replace the damaged tissue by integrating with the problematic part of the body in order to increase the life expectancy (14) .The diverse mechanical, physical, chemical, and structural properties of biomaterials allow them to be used in various applications depending on the biocompatibility and characteristics. Ceramics are a class of biomaterials used in biomedical devices(15). Ceramics are widely used as implant materials owing to their ability to be fabricated into a variety of shapes, along with their high compressive strength, variable porosity, and bioactive properties in the body (16) .The high similarity in the chemical composition of some ceramics such as calcium phosphate with human bone minerals makes them suitable for use as orthopaedic implants (human skeleton, bones, and joints), and dental materials (17). These materials show excellent bioactivity, high biocompatibility, and excellent osteoconduction characteristics (18) .Repair of bone defect due to chronic disease or trauma still remains a challenge for clinicians. Above the critical size, the restoration of bone defect normally requires use of synthetic biomaterial(19). Due to the restricted supply of autologous bone and threat of possible infection from using allograft, it is necessary to use the synthetic biomaterial or xenograft, a bone segment from different animal species (18, 20). Benefit of using xenogenous bone

is that it is very similar in structure and morphology to human bone. Xenografts such as bovine, sheep, pig, or fish bones contain trace number of beneficial ions, which are readily available in large supply and require low-cost processing (21). Xenogenous bone first undergoes a deproteination process followed by calcination at elevated temperatures.

1.5 Calcium Phosphates

Calcium phosphates are crystalline ceramics with a structure and chemical composition similar to minerals found in bone. An example of calcium phosphate widely used is HAp, which is represented by the chemical formula ($Ca_{10}[PO_4]_6[OH]_2$); it has a structure similar to the main mineral found in bone, apatite (22).

HAp is available as a bone filler and as coatings on prostheses, owing to its good biocompatibility, bioactivity, high osteoconductive and/or osteoinductive capacity, nontoxicity, noninflammatory behavior, and nonimmunogenic properties(23).Calcium phosphate scaffolds are described as promoting osteogenesis and osteointegration, which seems to be related to surface charge and the chemistry and topography of the scaffolds(24). However, this ceramic has a low resorption rate. Therefore, other calcium phosphates, such as β-tricalcium phosphate, which have fast resorption rates, have been studied. As an alternative, new sources of calcium phosphate have been explored (Fig1.1). Calcium phosphates can be extracted from different marine origins such as fish bones, corals, seashells, and algae. Sponges from the phylum Porifera have been explored because their skeleton is composed of bioceramics, and new methods have been developed to assess the overall regenerative and mineralogenic performance in zebrafish. HAp has been extracted from the porous exoskeleton of corals owing to

its similarity to bone and its mechanical, osteoconductive, and resorbable properties (25). This interesting material can be found commercially, such as in Pro Osteon 200R (Biomet), an osteoconductive bone graft (26).

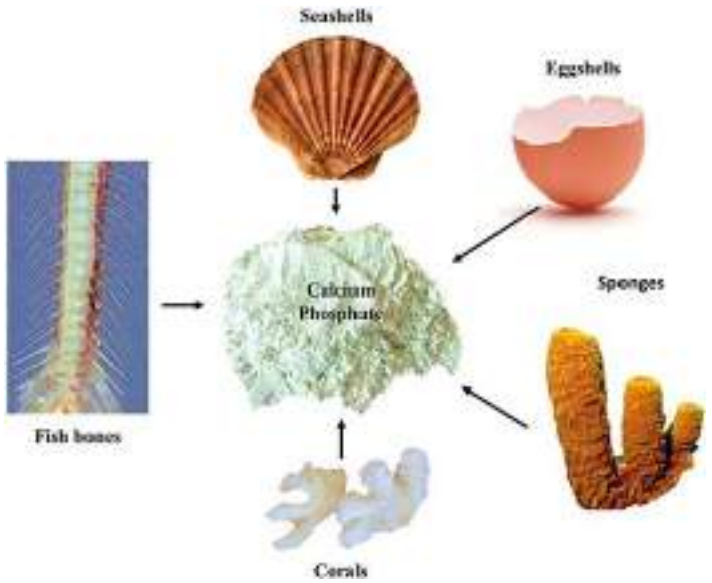

Figure 1.1: Some sources of calcium phosphate.

1.6 Hydroxyapatite (HA)

HA, as its name suggest, is the hydroxylated representative of phosphate minerals known as apatites (HA chemical formula: $Ca_{10}(PO_4)_6(OH)_2$. These bioceramics crystalize into the hexagonal system (Figure 1.2) (27), and can be artificially synthesized by different methods, including precipitation, hydrothermal, multiple emulsion, biomimetic deposition, and electrodeposition techniques (28) .Also, HA powders and coatings have been successfully synthesized by the sol gel approach, in which a number of combinations between calcium and phosphorus precursors are mixed to produce a high pure HA at molecular levels (28, 29). Considering all the efforts that have been made to optimize its synthetic production, HA can also be extracted from bone matrix, where it is naturally found in abundance. Indeed, 60-70% of the acellular bone matrix consists of its inorganic components, which provide its significant mechanical strength (30). Natural HA exhibits a Ca/P ratio higher than 1.67 and its non-stoichiometric nanostructured crystal contains carbonate groups and traces of different ions such as HPO^{2-}_4, Na^+, Mg^{2+}, Sr^{2+}, K+, Cl− and F− within its structure(31).

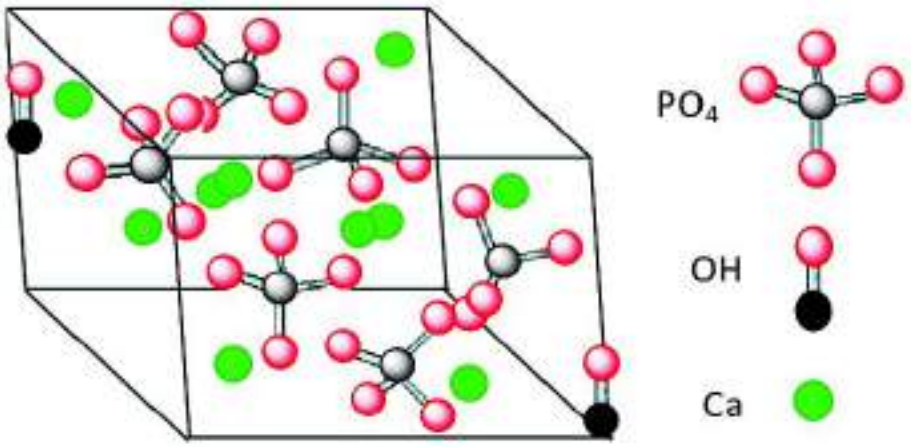

Figure 1.2: Crystal structure of hydroxyapatite

1.7 Hydroxyapatite and related compounds

Calcium phosphate (CP)-based biomaterials are group of compounds having Ca/P molar ratio in the range of 0.5–2 (32) and are the most sought-after biomaterials for the reconstruction of various bone defects especially in the field of dentistry, orthopedic and trauma surgery (33, 34). A brief list of important CP-based ceramic materials along with their formulas and applications is presented in Table 1. Due to exceptional biocompatibility (35, 36) osteoconductivity (37), and osteointegration (38), CP-based materials have been under intense investigation for over half a century. These CP-based biomaterials have been successfully used to replace and augment damaged, worsened, or degenerated hard tissues of the human body(39).

Apatite is the general name used for CP class of minerals and have general formula $A_4B_6(MO_4)_6X_2$, where A and B are considered as calcium in many living tissues, MO_4 is designated as phosphate group, and X indicates the presence of OH- group in the apatite structure(40). HA is an important CP-based material, which resembles mineral component of natural bones and teeth (41). HA with Ca/P ratio of 1.67 exhibits exceptional biocompatibility (42) and bioactivity (43). It has been used as a bone substitute material (44) and dental implant for over 50 years. HA can promote rapid bone regeneration and direct bonding with regenerated bone without the need of intermediate connective tissues and its synthetic form is mostly applied to reconstruct the hard tissue due to its osteoconductive properties(45). Due to the growing importance of HA as a biomaterial, continuous attempts are being made to enhance the biological properties of HA. Although HA crystals are frequently used in orthopedic field, its high dissolution rate in the physiological atmosphere limits its applications in the medical field(46). Research has shown

that the dissolution rates of HA can be altered by incorporating biocompatible ions into its ion-friendly crystal structure (47).

Table 1.1: Important calcium phosphate compounds with ratio Ca/P and PK_s[a]

No.	Compound	Formula	Ellipsis	Ca/P ratio	-log (Ks)	Application
1	Monocalcium phosphate monohydrate	$Ca(H_2PO_4)2.H_2O$	MCPM	0.5	1.14	Increase root fluoride uptake[7]
2	Monocalcium phosphate(anhydrous)	$Ca(H_2PO_4)_2$	MCPA	0.5	1.14	Artifical bone graft
3	Dicalcium phosphate anhydrous	$CaHPO_4$	DCPA	1	6.90	Polishing agent for teeth,source of Ca and P in food supplements
4	Dicalcium phosphate dihydrou	$CaHPO_4.2H_2O$	DCPD	1	6.59	Sustained release of highly water-soluble drugs[8]
5	α- Tricalcium phosphate	$\alpha\text{-}Ca_3(po_4)_2$	α-TCP	1.5	25.5	Biodegradabie composite for bone repair[9]
6	β- Tricalcium phosphate	$\beta\text{-}\ Ca_3(po_4)_2$	β- TCP	1.5	28.9	Orthopedic surgery
7	Calcium-deficiient hydroxyapatite	$Ca_{10-x}(HPO_4)_X(PO_4)_{6-X}$	CDHA	1.5-1.6	85	Bone grafting
8	hydroxyapatite	$Ca_{10}(po_4)_6(OH)_2$	HA	1.67	116.8	Repairing of hard tissues
9	Fluorapatite	$Ca_{10}(po_4)_6\ F_2$	FAP	1.67	120	Used as source of fluorine pharmaceutical products
10	Tetracalcium phosphate	$Ca_4(po_4)_2\ O$	TTCP	2	38-44	Applied as cements and coatings on metallic implants

Hydroxyapatite, HAp ($Ca_{10}(PO_4)_6(OH)_2$), is thermodynamically stable in its crystalline state in body fluid and has a very similar composition to bone mineral(48). HAp can integrate with bone without causing any local or systemic toxicity, inflammation or foreign body response(49). For these reasons, HAp has been widely used for biomedical applications particularly in orthopedic, odontology, and as the coating material for metallic implants (20, 50). Consequently, methods for synthesizing HAp with customizable characteristics have been extensively studied. Although many synthesis methods have been developed, the preparation of HAp with specific characteristics still remains challenging because of the possibility of formation of toxic intermediary products during the synthesis of HAp (51). Therefore, studies on new parameters of synthesizing HAp are still ongoing. HAp can be synthesized chemically or extracted from natural sources. Prior research has reported on the various methods for synthesizing and natural HAp (52). The review by Sadat-Shojai et al. concluded that synthetic HAp can be fabricated through various methods including dry methods (solid-state and mechanochemical), wet methods (chemical precipitation, hydrolysis, sol-gel, hydrothermal, emulsion, and nonchemical), and high temperature processes (combustion and pyrolysis) (53). Most conventional chemical methods involve the synthesis of HA without any trace of beneficial elements such as Na^+, Zn^{2+}, Mg^{2+}, K^+, Si^+, Ba^{2+}, F^-, $CO_3^{\ 2-}$, etc.; the presence of these ions directly influences various biochemical reactions linked with the bone metabolism. Recently, many research articles have been devoted to the synthesis, characterization, and application of ion-substituted HA(54). Ions can replace the Ca ions inside the crystal structure or can replace either the OH^- or the PO_4^{3-} ions, which is usually referred to as A-type or B-type substitution, respectively. Extraction of HA and its precursors from inexpensive natural biological reservoirs such as mammalian and fish bones(55), corals, eggshells, sea shells, and plants has opened up attractive and efficient means of preparing ion-doped HA(56).

1.8 Natural hydroxyapatite

Natural hydroxyapatite is usually extracted from biological sources or wastes such as mammalian bone (e.g. bovine, camel, and horse), marine or aquatic sources (e.g. fish bone and fish scale), shell sources (e.g. cockle, clam, eggshell, and seashell), and plants and algae and also from mineral sources (e.g. limestone). Fig1.3 shows the sources and examples of techniques used for synthesizing natural HAp(57). Stoichiometric HAp is basically composed of calcium and phosphorus with molar ratio of Ca/P equal to 1.67 (58). This ratio has been proven to be the most effective in promoting bone regeneration (53, 59). Natural HAp is non-stoichiometric and is either deficient in calcium or phosphorus. Calcium positions are the most common vacancy in HAp where cations such as Na^{+}, Mg^{2+}, and Al^{3+} are substituted in the calcium positions(60), while carbonate ions can substitute for either phosphate or hydroxyl ions while fluoride ions substitute for hydroxyl ions (37).

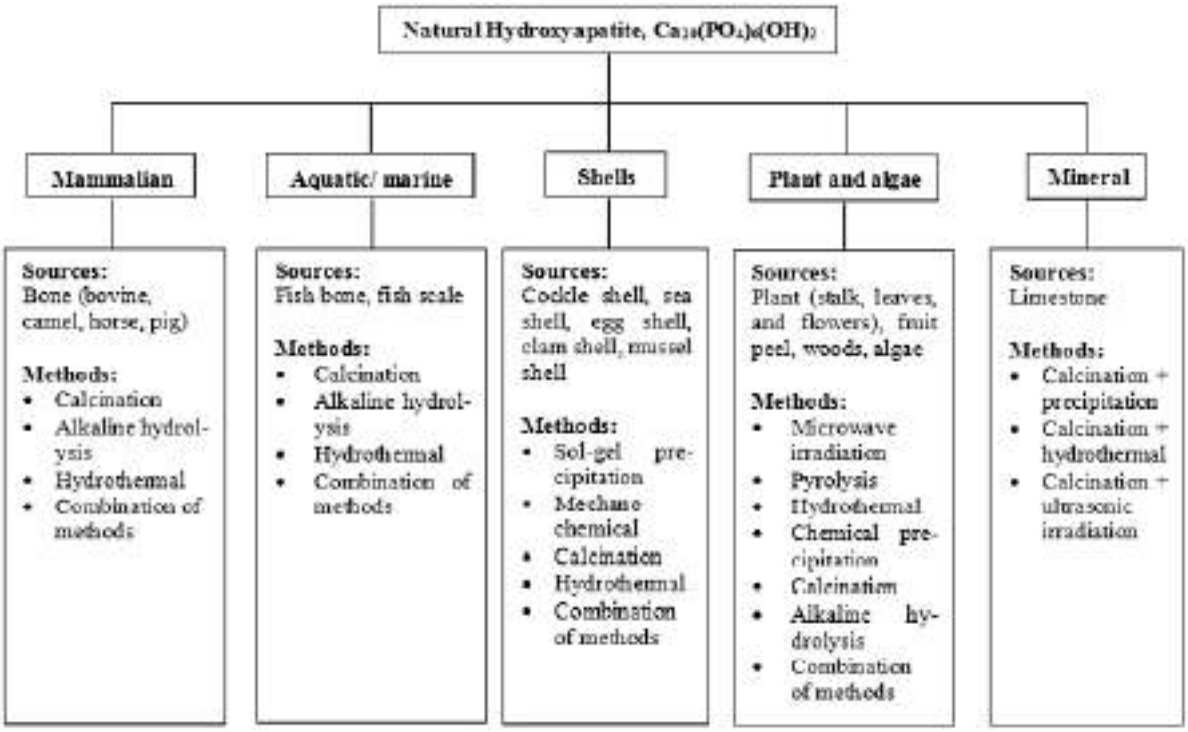

Figure 1.3: Summary of processes for synthesizing natural HAp.

The usage of HAp extracted from natural sources can be considered to be an environmentally friendly, sustainable, and economical process to fabricate these materials since these materials are available in large quantities. This can result in positive contributions to the economy, environment, and to general health.

1.9 Biological sources for the synthesis of hydroxyapatite

1.9.1 Extraction of hydroxyapatite from mammalian bones

Among mammalian sources, the extraction of HAp from bovine bone was frequently reported in literature compared to other sources such as camel, horse and, porcine. The cortical part of the femoral bone is usually used because they are morphologically and structurally similar to human bone (61). Reviewing the literature shows that the properties of the extracted HAp, such as the Ca/P ratio, size, shapes and crystalline phases of Ca-P have been discussed. These properties differ with the applied extraction methods and thus the parameters such as calcination temperatures and PH(58). Generally, most literature have reported that pretreatment of the bone is usually done before proceeding with the extraction method(41). The pretreatment involves washing and removing the dirt, fats, protein, and other components such as bone marrows and soft tissues. Some literature reported the usage of boiling water to remove organic components from the bone by boiling for times of 8 h or more (62). A combination of boiling and washing with solvents such as acetone and chloroform have been employed for the pretreatment of bone (63). Another pretreatment method that has been widely used is washing the bone alternatively with surfactant and alkali solutions to remove the soft tissues and decellularize it (43). The bone was also cut into smaller pieces before or after removing the organic constituents. Most majority of literature reported that the bone was cut first into smaller pieces before boiling or treated with the solvent to remove the unwanted components such as bone marrow located inside the bone(43, 64). most of the methods for extraction of HAp from mammalian bones used the calcination method which is either the sole process or a combination of calcination with other methods. The calcination process involves heating the bone in a furnace at

different temperatures of up to 1400 °C in order to completely remove the organic matter and kill the pathogens which may be present (65).

Barakat et al. employed the alkaline hydrothermal hydrolysis treatment to extract HAp from bovine bone (66). The extracted HAp was heated to 250 °C for 5 h resulting in the formation of nanoflake HAp with Ca/P ratio of 1.86. They also reported that nanoflake HAp with Ca/P ratio of 1.56 could be produced using subcritical water process (67).

1.9.2 Hydroxyapatite from bovine bone

Hydroxyapatite extracted from bovine cortical bone has been used to fabricate HA/collagen (extracted from bovine tendons) scaffolds for tissue engineering purpose Extracellular matrix in bovine bone is mainly composed of HA nanocrystals and collagen fibers and, therefore, has been a focus of numerous studies exploring the extraction of natural HA(68). Extraction of HA from natural bone materials is economically viable and easy to carry out. Bone is inimitable composite matrix of collagenous fibers (20 wt%), apatite minerals (69 wt%), water (9 wt%), and organic matters such as proteins, lipids, and polysaccharides are present in small quantitiesn (69). Thermally stable phase-pure HA was produced by calcinating bovine femur, sheep femur bone, sheep skull flat bone, and chicken femur bone between 600 and 1100 °C (70). The calcination process at 800 °C produced phase-pure crystalline HA having crystallite size around 133 nm with trace amounts of Na^{+}, Mg^{2+}, Sr^{2+}, and K^{+} with Ca/P between 1.46 and 2.01(57). Increase in calcinations temperature to 1100 °C increased the crystallinity of the HA but this high calcination temperature resulted in the formation of β-TCP. XRD spectra of bone heat-treated at 1100 °C matched perfectly with the standard XRD pattern of crystalline HA (JCPDS card No. 9-432),

while Scherrer equation was used to calculate the average crystallite size (58.4 nm). The presence of secondary phases such as CaO and $Ca(OH)_2$ was attributed to the lack of incubation of bone-derived mass with 1 % phosphoric acid after calcination at elevated temperature(59). Phase-pure crystalline HA can be extracted from bovine bone using alkaline hydrothermal hydrolysis of organic matrix at 250 °C, subcritical water extraction of collagen at 275 °C, and most commonly used thermal decomposition of collagen and other organic matter at 750 °C (71). All three extraction methods produced phase-pure HA but the morphology and particle size were directly influenced by the extraction process employed. Effect of sintering temperature (500–1400 °C) on physical and chemical properties of bovine bone-derived HA revealed that 1000 °C sintering temperature is sufficient to produce HA; however, XRD results confirmed the dehydroxylation of HA during sintering at temperatures above 1000 °C (72). EDX results confirmed the formation of calcium-rich (Ca/P = 1.85) HA phase, which was attributed to the presence of Na^+ and Mg^{2+} ions observed in the EDX spectra(73).

Other methods such as alkaline heat treatment have been used to extract HAp from mammalian bone. In this method, the alkaline solution usually NaOH is used to remove the organic matter from the bone. The NaOH solution hydrolyzes the organic component in the bone and the remaining calcium phosphate is rinsed and separated using filtration. However, alkaline heat treatment produces low crystallinity HAp compared to calcination(71). Sun et al revealed that the crystallinity of HAp produced using alkaline heat treatment was much lower than that seen for calcined HAp (74).

1.9.3 Hydroxyapatite HAp from fish bone

Calcium phosphates can be prepared by using either natural organic or inorganic raw materials. Fish bone is considered as a one of the potential biological sources to produce calcium phosphates(75). Various fish bones from anchovy (Engraulisencrasicolus),barramundi(Latescalcarifer),carp(Cyprinuscarpio), cuttlefish (Sepiaofficinalis),croaker(Micropogoniasundulatus),cod(Gadusmorhua),congereel (Congerconger),(Fig.1.4) flatfish(Heterosomotapleuronectiformes), flying fowl, greater amberjack (Seriola dumerili), mackerel (Trachurus trachurus), lizard, sardine (Sardina pilchardus), shark, sier, sea bass (Dicentrarchus labrax), sea bream (Sparus aurata), sheelavati, swine, sword fish (Xiphias gladius), tilefish (Lopholatilus chamaeleonticeps), trigger fish (Balistoides viridescens) and tuna (Thunnus albacares) have been used as a starting material to produce HA and β-TCP as listed in Table 1(76). There are several methods to prepare calcium phosphates from fish bone (77-81).

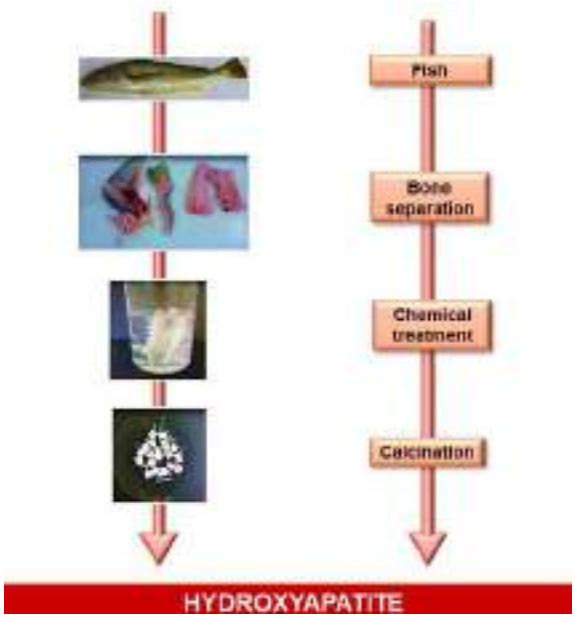

Figure 1.4: Chemical steps for extracting hydroxyapatite from fish.

1.10 Future Perspectives

Recent data regarding the use of HA from fish for tissue engineering, focusing on studies concerning its physical-chemical properties and biological response. These findings suggest that (82), supporting cell growth in vitro, with a low risk of transmission of infection-causing agents as far as good biocompatibility(83). In this context, HA from fish is a promising resource for bone tissue engineering with commercial interest, and for medical and dental products (Figure 1.5). However, some limitations and challenges for their use should be overcome. Among them, all biocompatibility tests should be conducted through in vitro and in vivo studies using different species of fishes in order to determine the safety and efficiency of the material. Furthermore, different forms and presentation of HA from fish should be manufactured and tested. Recent studies have demonstrated that nano-sized HA can mimic better dimensions the components of bone tissue(84). Thus, nano-HA fish-based biomaterials may present the same advantages of nano synthetic HA, offering a better bioactivity and dissolution than coarser crystals due to large surface to volume ratio and unique chemical properties(85). Therefore, it is expected that nanoHA from fish would promote increased osteoblast adhesion and cell proliferation(86).

Figure 1.5: Fish, hydroxyapatite and clinical application.

1.11 Thermal calcination method of HAp

The thermal calcination route, a traditional method, can serve as a straightforward approach to produce HA and β-TCP from fish bones(87). The calcination temperature, calcination time, extraction method, and nature of bones are among the factors affecting the final properties of calcium phosphates such as Ca:P ratio, morphology, phase purity, size distribution and surface area (88). A general flow diagram of calcium phosphate extraction from fish bone is given in Fig. 6. Synthetic HA and β-TCP are stoichiometric materials with calcium to phosphorous molar ratio of 1.67 and 1.50, respectively (20). The Ca/ P ratio of HA and β-TCP derived from natural sources differed from stoichiometric Ca/P molar ratio depending on the availability of trace elements (28, 89). There are studies showing that chlorine (51) copper ,fluorine, iron, magnesium, manganese ,potassium, silicon, sulfur, sodium, strontium and zinc existed as minor components among the major components (calcium, phosphorus) (59, 90).

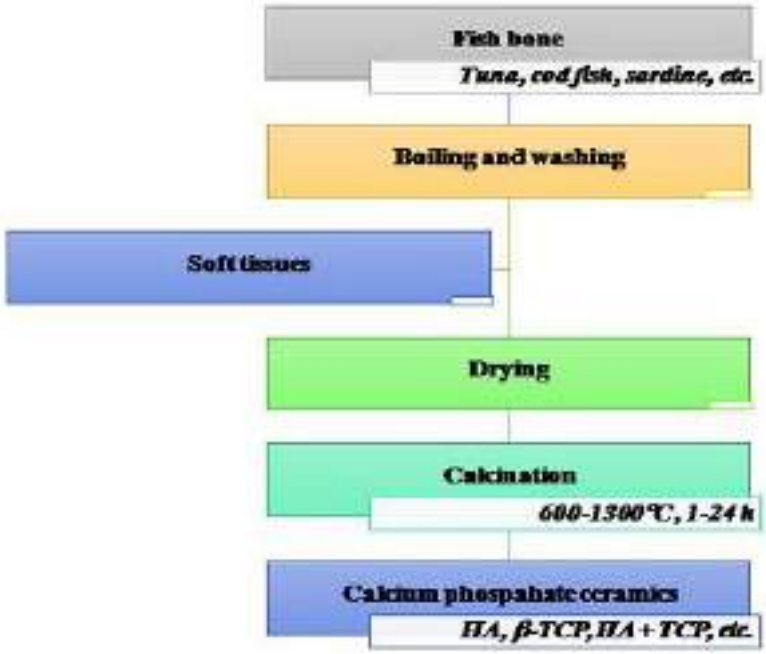

Figure 1.6: General flow diagram of calcium phosphate extraction from fish bones

The increasing consumption of fish around the world has caused significant increase in fish waste production in the form of scales and bones. The recovery of fish scales and bones allows for extraction of HAp and reduction in solid wastes in the fisheries industry (91). The fish bone is rich in calcium, phosphate, and carbonate which make it a great source for extraction of HAp. Therefore, Marine waste has been exploited to prepare various bioactive compounds. Caught fish is typically used to provide fish meat, fish oil, and some low economic value fertilizers. However, recent research studies have identified the presence of several CP salts in these sources; therefore, they are being exploited to prepare bioactive compounds (91). Fish bones are a rich source of calcium, phosphate, and carbonate which can be used to prepare HA. These bioactive compounds can be synthesized using different simple to complex techniques. Generally, fish bones are used to extract calcium for various dietary products; however, very little attempts have been made to synthesize HA from these natural sources for biomedical application (92). In order to convert fish bones or related sources into HA, these bones are washed with hot water or steam or different alkaline solutions to remove all types of proteins and other organic impurities. After the removal of protein mass, the bones are subjected to high-temperature calcination to furnish HA. Hydroxyapatite particles having size around 300 nm and spherical in shape were synthesized from the bones of Hydroxyapatite particles having size around 300 nm and spherical in shape were synthesized from the bones of Brazilian river fish such as pentado (Pseudoplatystoma corruscans), jau´ (Paulicea lutkeni), and cachara (Pseudoplatystoma fasciatum) (93). Fish bones were initially calcined at 900 C for 4–12 h followed by the crushing of bones with high-energy ball mill for 2 and 4 h. SEM analysis indicated that the milling time affected the size of spherical particles. Elemental analysis confirmed the presence of Fe^{2+}, Cr^{3+}, Ni^{2+}, Mn^{2+}, Cu^{2+}, Zn^{2+}, K^{+}, and Na^{+} as trace elements; however, the presence of

first four ions was attributed to the use of stainless-steel milling balls. Synthesis of phase-pure nanocrystalline cHA from Fish (Tilapia nilotica) scale waste through alkaline heat treatment method was reported recently (94). Thoroughly washed and dried fish scales were deproteinized and heated with 50 % sodium hydroxide at 100 C for 1 h to furnish HA. FTIR analysis confirmed the replacement of some of the phosphate groups with the carbonate group (B-type substitution). ICP-OES confirmed that the Ca/P ratio was 1.67, same as the theoretical value (95). Porous HA with Ca/P ratio of 1.78 was extracted from washed and crushed tilapia (Oreochromis sp.) fish scales using enzymatic hydrolysis with 1 % protease N followed by hydrolysis with 0.5 % flavoenzyme solution(96). The extracted HA appreciably promoted the cell viability of MG63 type when compared with commercially available HA. This enhanced biological activity was attributed to smaller particle size (719.8 nm). Thermal extraction of HA from Cod fish bones by annealing the raw bones at temperatures between 900 and 1200 ^{o}C was reported recently (97). The morphological analyses of the HAp extracted from the mammalian bone show that the particles are mostly irregular in shape, with some studies showing the presence of rods, flakes, needles, and plate-like shapes. Thus, the shape variation is believed to not be affected by the method or source. For example, calcination of same source of bone could produce the various shapes of HAp such as rod-like, spherical, and needle like(98). In addition, the rod shape HAp could be produced using different extraction methods such as alkaline hydrolysis and combination method. It can be concluded that, there is no relation between the morphology of HAp with the extraction method and source (7). The size of HAp obtained did not show any correlation with the extraction method. The use of additional milling helped to reduce the size of the HAp particles to the nanometric size which is close to that of human HAp(99). In addition, the nanosized particles have advantages in terms of high surface activity and ultrafine structures (100).

1.12 Alternative preparation method

Researchers have conducted studies on the calcium phosphates production with alternative methods such as alkaline hydrolysis, hydrothermal and laser ablation (Fig1.7). Synthesis of blue shark (Prionace glauca) fish bone-based microscale particles by using laser ablation system combined with a compressed gas jet without previous calcination was reported (101), The extracted micro and nanoscale particles were composed of HA whitlockite ($Ca_3(PO_4)_2$) and HA. The study showed that it is possible to obtain calcium phosphates by direct ablation method without calcination. The preparation of calcium phosphate nanoparticles extracted from calcined sword fish bones, by means of laser ablation in de-ionized water was studied (92). Fish bones were firstly calcined at 950 °C to prevent any potential organic impurity and then milled to obtain micro sized particles. The hydroxylapatite micro particles were used as precursor material in laser-induced fragmentation tests. Hydroxylapatite and β-tricalcium phosphate nanometric particles were obtained with 10 nm diameter. In another study, Boutinguiza et al. (102). Were used CO_2 pulsed laser ablation to obtain calcium phosphate nano size particles from sword fish bones previously calcined at 600 °C. The amorphous and spherical particles were obtained with a mean diameter of approximately 25 nm(103).

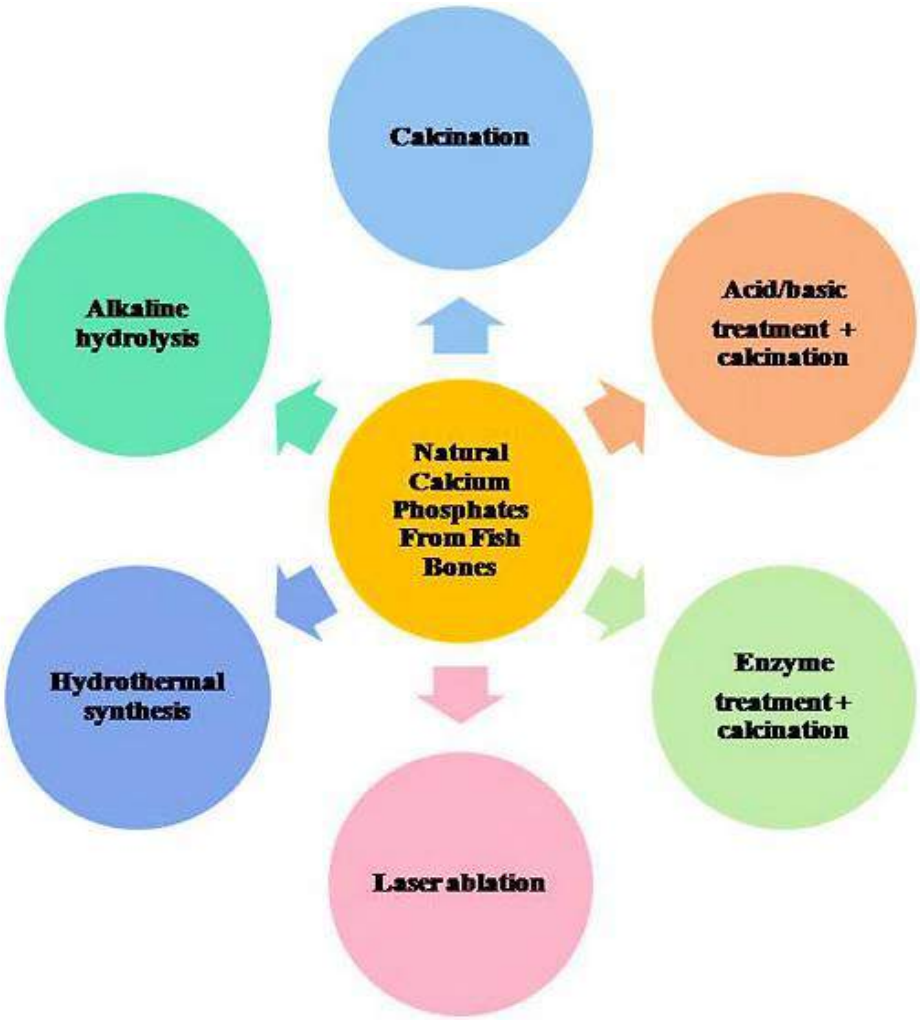

Figure 1.7: Fish bone derived calcium phosphate production methods

1.13 Antibiotics

Major attention has been paid to antibiotics, due to their wide areas of application: either as prophylactics to prevent infections produced during surgical interventions, or in general in the treatment of bone infections(104). In fact, one of the key factors for the success of surgical interventions aimed at the implantation of a prosthesis or of an osteoconductive material is the prevention from bacterial infections(105). Wound contamination, or postoperative infections following fracture repair, implantation of joint prosthesis or spine surgery, can cause serious problems (106). For this reason, antibiotics are often provided as prophylactics, either orally or intravenously. However, the little accessibility of the site of infection to antibiotics delivered systemically lengthens often the treatment of bone infections over 1 year (107).

In order to reduce the incidence of implant-associated infections, several biomaterial surface treatments have been proposed. Previous works on conferring antibacterial property to biomaterials have relied on surface functionalization techniques, such as coating of implant surfaces with silver ions (108). Regardless of these findings, it is also known that there are different forms of Ag that confer bactericidal properties to different degrees. The antimicrobial properties of Ag^+ ions have been exploited for a long time in the biomedical field Ag^+ ions are considered to have a broad spectrum of antimicrobial properties(109), which is of significance for the bacterial colonisation associated with biomaterial related infections (110).

1.14 Research Background

HA is a well-known due to its chemical similarity with the natural hard tissue and excellent biocompatibility. However, HA is poorly soluble under physiological conditions and can remain in the body for years without significant signs of resorption. Many studies have reported extremely slow biodegradation, where HA has been detected through X-rays after many years of implantation (Figure 1.8).

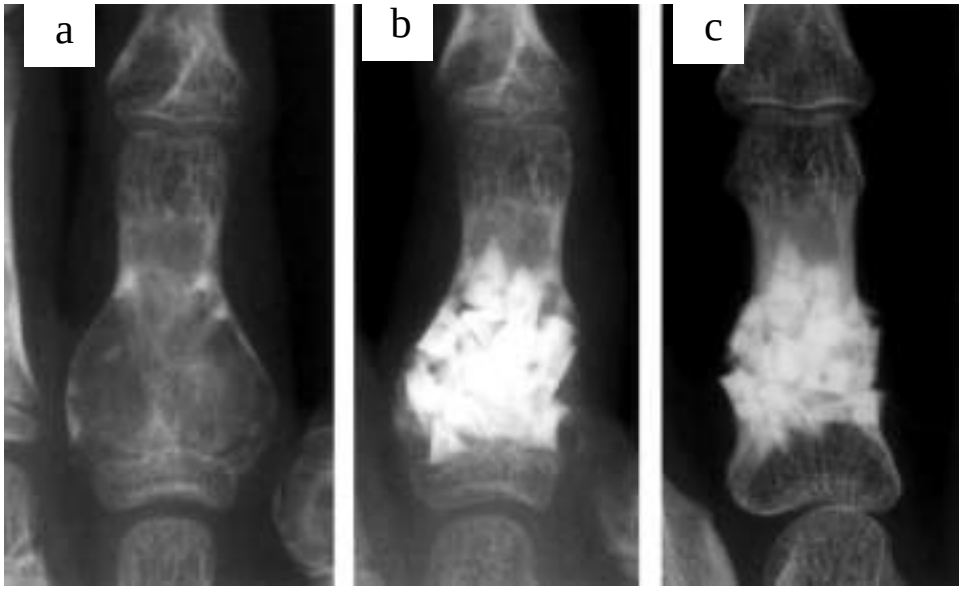

Figure 1.8: Radiographs of (a) extensive growth of the tumour with thin cortex, (b) clear margin of the implanted HA one month after operation, and (c) absorbed margin of the HA less than 50% 11.6 years after operation with remodelling of the deformity of the metaphysis.

1.15 Problem Statements

Most conventional chemical methods involve the synthesis of HA without any trace of beneficial elements such as Na^{+}, Zn^{2+}, Mg^{2+}, K^{+}, Si^{+}, Ba^{2+}, F^{-}, $CO_3^{\ 2-}$, etc.; the presence of these ions directly influences various biochemical reactions linked with the bone metabolism. Although many synthesis methods have been developed, the preparation of HAp with specific characteristics still remains challenging because of the possibility of formation of toxic intermediary products during the synthesis of Hap. Therefore, studies on new parameters of synthesizing HAp are still ongoing. HAp can be synthesized chemically or extracted from natural sources. Extraction of HA and its precursors from inexpensive natural biological reservoirs such as mammalian and fish bones.

The fish bone is rich in calcium, phosphate, and carbonate which make it a great source for extraction of Hap. Fish bones are a rich source of calcium, phosphate, and carbonate which can be used to prepare HA. These bioactive compounds can be synthesized using different simple to techniques. Generally, fish bones are used to extract calcium for various dietary products; however, very little attempts have been made to synthesize HA from these natural sources for biomedical application.

1.16 Objectives of the Study

1. The effect of extraction process and natural waste source on the critical properties of the HAp such as Ca/P ratio, crystallinity and phase assemblage, particle sizes, and morphology.
2. Highlights the importance of extracting HA from natural resources and gives future directions to the researcher so that HA extracted from biological resources can be used clinically as a valuable biomaterial.
3. *In-vitro* bioactivity will be studied by immersing the samples in the SBF solution and anti-bacterial performance will be monitored through quantitative and qualitative analysis.
4. To explore extracting HA as drug carriers for sustained drug release applications

1.17 Scope of the study

In this study a simple and cheap method is presented, based on heat treatment to produce great amounts of HA from natural sources. These materials present a promising future because the raw material are wastes, while using a biological substituted apatite containing Mg and Sr as bone substitutes, instead of synthetic apatite without them, would be much beneficial for bone defect healing. Overall, these results confirm the suitability of these materials for biomedical applications.

1.18 Significance / Novelty of the study

The goal of this study is to synthesize HAp from the natural sources. The main objective of our study was to find out an available source for extraction of HA in aspect of our country. Therefore, the objective of this study was to pinpoint the preparation and characteristics of natural HAp produced natural sources using a high heat treatment (900, 1000°C). The Ca/P molar ratio was determined to be 1.67 which is the stoichiometries HAp. These findings have potential as a biomaterial for biomedical applications. The extracted of materials proposed in this study is a modest effort to produce bioactive materials in Iraq, which will significantly reduce their cost and make them available to the ordinary citizens at affordable rate.

CHAPTER TWO

METHODOLOGIES

2.1 Materials and Chemicals

All chemicals used for synthesis were reagent-grade and were used as received.

The Simulated body fluid (SBF) to evaluate the *in vitro* bioactivity was prepared according to the method of (Kokubo 1990) (Table 2.1) (111). Simulated body fluid (SBF) solution was prepared according to previously reported methods Specifically, a solution consisting of NaCl, $CaCl_2$ $NaHCO_3$, KCl, $K_2HPO_4 \cdot 3H_2O$ $MgCl_2 \cdot 6H_2O$, and Na_2SO_4 in distilled water was mixed with HCl to arrive at a pH value of 7.4. Our specimen was soaked into 20 mL SBF solution in a water path at 37°C.

Table 2.1: Ionic composition of SBF and human blood plasma

Ions	pH*	Na^+	K^+	Ca^{2+}	Mg^{2+}	Cl^-	HCO_3^{3-}	HPO_4^{2-}	SO_4^{2-}
SBF (mM)	7.4	142.0	5.0	2.5	1.5	147.8	4.2	1.0	0.5
plasma(mM)	7-7.4	142.0	5.0	2.5	1.5	103.0	27.0	1.0	0.5

*The pH of SBF is adjusted by using tris-hydroxy methylamino methane $(CH_2OH)_3CNH_2)$ buffer solution and 1M HCl.

All chemicals that are used to prepare SBF are purchased from (QREC, Auckland, New Zealand).

2.1.1 Equipment and Apparatus

In this study. The following apparatus and equipment were used.

Table 2.2. Apparatus used during the study period with the name of the Manufacturer and the country of Origin

NO.	Equipment and apparatus	Company \ origin
1	X-Ray Diffraction (XRD)	Philips PW1730
2	FTIR spectrophotometer (spectrometer)	Nicolet iS50
3	Field Emission Scanning Electron Microscope (FESEM)	Zeiss-LEOModel1530
4	Energy Dispersive X-Ray Analysis (EDX)	Oxford instrument, Swift ED 3000
5	UV-Vis Spectroscopy	UV-3101PC; Shimadzu, Tokyo, Japan)
6	Flame Atomic Absorption Spectrometer (Perkin Elmer A Analyst 400).	(Perkin Elmer A Analyst 400).

2.2 Chemicals

Table 2.3. All Chemicals Used in the study with the Name of the Company Manufacturer and Country of Origin.

NO.	Chemicals	Company/origin
1	Aceton	Sigma Aldrich
2	Petroleum ether	Sigma Aldrich
3	Potassium chloride	QREC, Auckland, New Zealand
4	Sodium chloride	Sigma Aldrich
5	Potassium chloride	Sigma Aldrich
6	Sodium hydrogen carbonate	Sigma Aldrich
7	Potassium phosphate	QREC, Auckland, New Zealand
8	Magnesium di chloride	Sigma Aldrich
9	Hydrochloric acid	Sigma Aldrich
10	Calcium chloride	Sigma Aldrich
11	Sodium sulfate	QREC, Auckland, New Zealand

2.3 Samples Preparation

The calcination method used to obtain HAp from fish (Cyprinus Carpio) in south Iraq. Preparation of Bone Powder. method adopted for the extraction of HAp was the modified procedures of bone samples were cleaned to get rid of visible impurities employing a sharp knife. Were cut into small pieces using a hacksaw. Pieces were boiled for about 2 h in a closed container to remove macroscopic adhering impurities. Subsequently, the samples were washed multiple times with distilled water and later immersed in (acetone and ether 3:1) for 24 h to remove the invisible fat, were then dried in a hot air oven for 17 h at 120°C to avoid shoot formation during grinding. dried bone samples were crushed into small pieces using an iron mortar and pestle to obtain powders with 0.2 mm size rang.

The calcination process took place, and the raw powder was heated in furnace at temperatures ranging from 200 °C to 1000 °C at a heating rate of 5 °C/min in 5 h. Utilized the calcination method to obtain HA from see fish using different temperatures (200 °C, 400 °C, 600 °C, 800°C, 900°C and 1000 °C) for 2 h **.**Sheep bone and chicken bone samples was prepared using the same protocol as for Fish bone for extracting HAp.

2.4 In vitro study

2.4.1 Determination of ions release

HAp samples for the evaluation of the ion release were extracted. After the preparation, samples were allowed to set for 24 h at 25 °C. The set samples were immersed in SBF solution. The SBF solution had a chemical composition and concentration similar to the inorganic part of human plasma and was prepared by dissolving NaCl, KCl, $K_2HP_4.3H_2O$,$NaHCO_3$,$(CH_2OH)_3CNH_2$ $MgCl_2.6H_2O$,$CaCl_2$, and Na_2SO_4 reagents in deionized water in accordance with Kokobo's specification, and pH of solution adjusted at 7.25 by hydrochloric acid, HCl. The samples were kept in SBF at 37 ºC for various times 0 day, 1 day, 3 day 7 day and 14 day. Then, the whole volume of the SBF was extracted for measurement of its Ca^{2+}, content and then fed with fresh solution again. The Ca^{2+}, concentrations were determined by using Flame Atomic Absorption Spectrometer (Perkin Elmer A Analyst 400).

2.4.2 Determination of in vitro drug release profiles

Samples for the evaluation of in vitro antibiotic release from the HAp are prepared by placing the HAp containing antibiotic. After the preparation, samples are left to set for 24 h at room temperature. Three samples from every batch are immersed in 15 ml of SBF and incubated at 37 °C ± 0.5 °C. 2 ml aliquots of the solution are taken directly from the vessels after 30 min, 1 h, 2, 3, 4, 5, 6, 7, 8, 10, 12, 24, 48, 72, 186 and 336 h. The amount of anti-biotic released is examined by a comparison with a calibration curve for the individual anti-biotic made in SBF. Antibiotic content in dissolution medium is determined by using ultraviolet–visible spectroscopy .

2.5 Characterization

2.5.1 X-Ray Diffraction (XRD)

Phase purity and crystallinity of all the samples were determined by using X-Ray Diffractometer (XRD, Bruker D8) operated at 40 kV and 30 mA utilizing CuKα radiation, at a step size of 0.02° and step time of 1 sec, all the diffractogram were recorded between 20° -80° of 2θ angles.

The degree of crystallinity was calculated according to the fraction of crystalline phase available in the analysed volume from X-ray diffraction data using:

$$X_C = 1 - (V_{112/300} / I_{300}) \times 100\% \quad \textbf{(}\text{Equation 3.1}\textbf{)}$$

where X_C is the degree of crystallinity, I_{300} is the intensity of (3 0 0) reflection and $V_{112/300}$ is the intensity of the hollow between (112) and (300) reflections(112).

The average crystallite size was calculated using Scherrer's equation (Equation 3.2)

$$D = 0.9\lambda/\beta\cos\theta,$$

where D = crystallite size (nm), λ = wavelength of the X-ray used (nm), β = full width of the line at half of its maximum intensity in radians (FWHM),

θ = diffraction angle

For crystallite size calculations we used the FWHM at (002), (300), (222) and (310) reflections.

Calculation of lattice parameters *a*, *c* and cell volume (*V*) of ion substituted CaP structure were made using the unit-cell program of Holland and Redfern

The percentage presence of secondary phase in the samples was determined from relative intensity ratio of the corresponding major phases by using (Equation 3.3a ,b)

Presence of phase to be determined = Relative Intensity ratio of the phase x 100 (Equation 3.3a**)**

Relative Intensity ratio = Intensity of the major peak of the phase / ∑ Intensity of major peaks of all phases (Equation 3.3b**)**

2.5.2 Fourier Transform Infrared Spectroscopy (FTIR)

Presence of functional groups were confirmed by using FTIR spectrophotometer (Nicolet iS50 spectrometer) using KBr disc method, all spectra were recorded in the scanning range of 4000-400 cm^{-1} in transmission mode with 32 scans and resolution of 4 cm^{-1}.

2.5.3 Field Emission Scanning Electron Microscope (FESEM)

Morphology and microstructure of the apatite layer were studied by FESEM (Zeiss-LEOModel1530) attached with Energy Dispersive X-Ray Analysis (EDX) (Oxford instrument, Swift ED 3000) operated up to 20 Kv. Samples were gold or platinum coated prior to the analysis to avoid charge buildup. An EDX operating at voltages up to 15 kV was used to study the elemental composition of apatite layer formed during the immersion of samples in SBF. Readings at 5 different locations were recorded to calculate the average elemental composition.

2.5.4 UV-Vis Spectroscopy

The absorption spectra of antibiotic release from HAp loaded antibiotic samples are noted on Shimadzu 3101, UV-Vis-NIR spectrophotometer between 200-800 nm spectral ranges.

The absorbance is analysed by utilizing twofold monochromatic diffraction grinding framework and photomultiplier R-928 indicator with resolution of around 0.1 nm.

2.6 In vitro Antimicrobial Activity

Antibacterial properties of HAp loaded with antibiotic are investigated qualitatively and quantitatively against Escherichia coli (E.coli, ATCC 25922 strains) and Staphylococcus aureus as descried below.

2.6.1 Qualitative Analysis

The HAp loaded with antibiotic samples are evaluated qualitatively via powder diffusion method against Escherichia coli and Staphylococcus aureus. Nutrient agar plates are vaccinated with 1 mL of bacterial suspension containing around 105 colony developing units (CFUs)/mL microbes. The powder (0.1gm) is delicately put on the vaccinated plates and then it is incubated at 37 °C for 24 h.

2.6.2 Quantitative Analysis

The HAp loaded with antibiotic samples are evaluated quantitatively via viable count method against Escherichia coli and Staphylococcus aureus. The standard solution is prepared by blending 1 mL E. coli with 9 mL of LB (Luria-Bertani) potage and incubated at 37 °C for 24 h with trembling at 250 rpm. HAp loaded with antibiotic (0.1g) is autoclaved and blended with the standard solution. The prepared mixture (0.1 mL) is immunized on LB agar plates which are then incubated at 37 °C. Lastly; the number of colony developing units is tallied.

CHAPTER THREE

RESULTS AND DISCUSSION

3.1 Extraction of Hydroxyapatite (HAp) from Fish Bones

Using calcination method used to obtain HA from fish (Cyprinus Carpio) from Misan in south Iraq. Preparation of bone powder, The calcination process took place, and the raw powder was heated in furnace at temperatures ranging from 200 °C to 1000 °C at a heating rate of 5 °C/min in 5 h. Utilized the calcination method to obtain HA from fish using different temperatures (200 °C, 400 °C, 600 °C, 800, 900 and 1000 °C) for 2 h.

3.2 X-Ray Diffraction (XRD) Analysis

A phase investigation of the HAp was carried out with the assistance of XRD (Figure 3.1). Crystallization of HAp occurs successfully after calcination at temperatures between 900 and 1000 ºC. The peaks in the XRD pattern for HA were found to be located at the coordinates (26.12 º), (28.45 º), (31.15 º), (33.20 º), (34.28 º), (40.11 º), (46 v), (49.47 º), and (55 º), and it was determined that these peaks correspond to the (002), (210), (211), (300), (202), (310) and (222), (213), and (304) planes of crystalline HA. It has been determined that HA crystallizes in a hexagonal structure with the following lattice parameters: a = b = 9.416Å, c = 6.863Å, and cell volume =527.3 Å3. The diffraction peaks and lattice parameters were in good agreement with the standard phase of HA (JCDPS 09-432). Along with the main peaks of HA, a tiny peak at 30.71º was observed with an increase in the calcination degree to 1000 ºC, which could be attributed to the (0210) diffraction plane of β-tricalcium phosphate (β-TCP, JCDPS No. 09-0169). The β-TCP phase appears as a minor phase as a result of HAp decomposition at high temperatures, (113). Furthermore, no significant changes were observed in terms of lattice parameters, degree of crystallinity, or crystallite size (Table3.1).

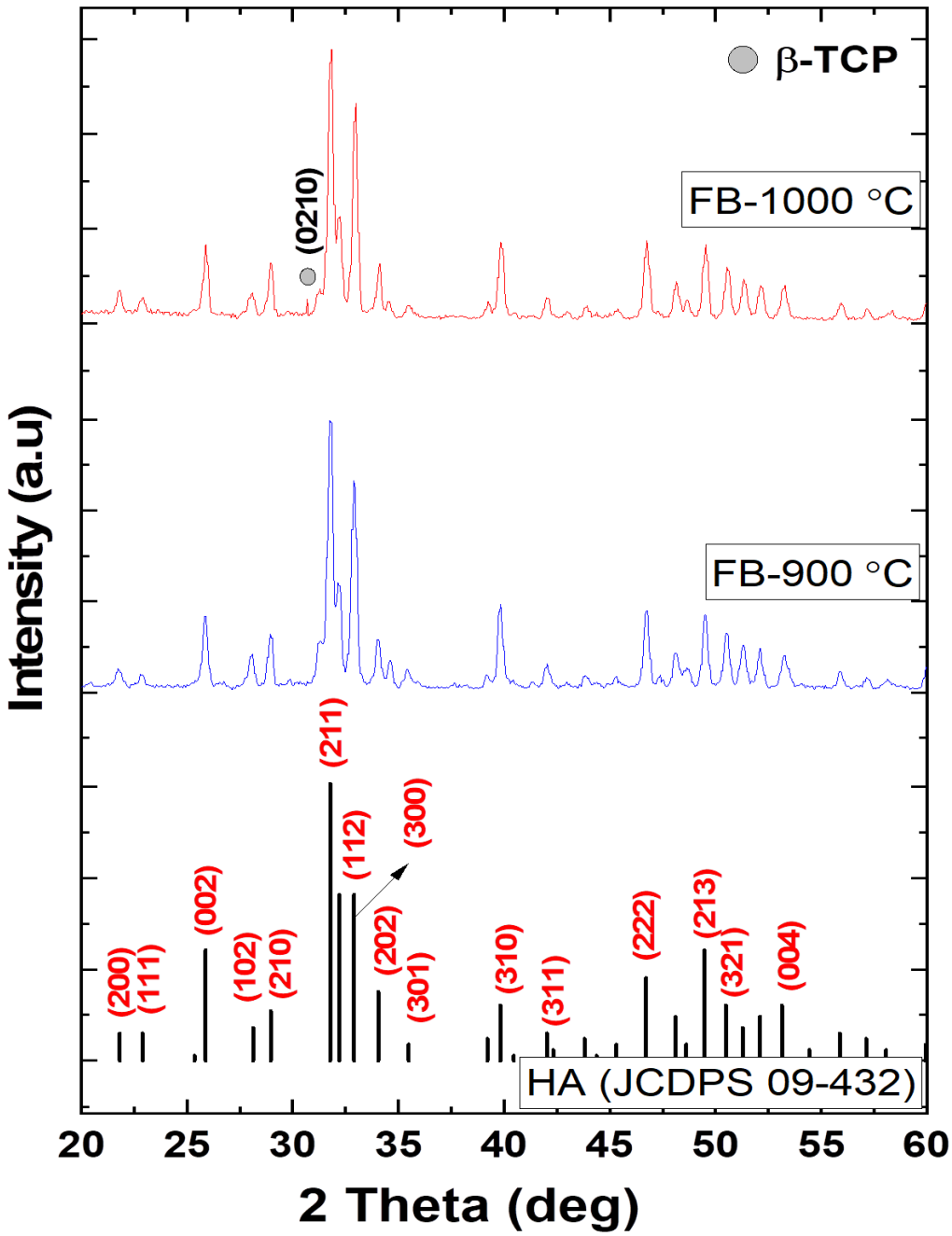

Figure 3.1: XRD pattern of fish bones calcined at 900 °C and 1000°C for 2 h.

Table 3.1: Lattice parameters, dgree of crystallinity and crystallite size of biological HA at 900ºC and 1000ºC.

Sample ID	Lattice Parameters			X_c (%)	*CS* (nm)
	a **(Å)**	***c*** **(Å)**	***V*** **(Å)^3**		
Standard HA	9.418	6.884	528.8	-	-
FB-900 °C	9.416	6.863	527.3	87.77	30.04
FB-1000 °C	9.417	6.860	527.1	79.31	53.79

- X_c = degree of crystallinity; *CS* = crystallite size.

Table 3.2: Peak List

Pos. [°2Th.]	FWHM Left [°2Th.]	d-spacing [Å]	Rel. Int. [%]
25.866940	0.246000	3.44446	28.06
28.039360	0.246000	3.18233	11.97
31.221560	0.196800	2.86486	16.78
32.223750	0.147600	2.77801	39.35
32.980290	0.246000	2.71600	58.58
34.034400	0.196800	2.63425	18.55
34.620570	0.196800	2.59098	10.88
39.158920	0.196800	2.30052	5.34
39.785350	0.246000	2.26573	28.66
41.978910	0.295200	2.15228	7.48
43.984990	0.590400	2.05866	3.22
45.308050	0.590400	2.00157	3.26
48.093880	0.246000	1.89194	13.39
48.735550	0.295200	1.86852	7.24
52.093730	0.196800	1.75570	15.11
53.237890	0.344400	1.72063	12.44
55.882890	0.246000	1.64530	6.41

3.3 FTIR spectra analysis

The presence of the functional groups in the extracted HAp was detected using FTIR analysis, and the results are shown in Figure (3.2)Four vibrational modes of the phosphate (PO_4^{3-}) group were recorded at 466 cm^{-1} (PO_4^{3-} (ν4), 565 cm^{-1} (PO_4^{3-} (ν2), 604 cm^{-1} (PO_4^{3-} (ν2), and 921-1200 cm^{-1} (PO_4^{3-} (ν1,3). The stretching and bending mode of hydroxyl (OH) group were observed at 3566 cm-1 and 634 cm^{-1}, respectively. Furthermore, the vibrational modes of carbonate

(CO_3^{2-}) were detected at 1406 cm^{-1} and 1514 cm^{-1}. The presence of carbonate groups is an indication of the formation of carbonated HAp. Nonetheless, it's possible that the presence of CO_3^{2-} really enhances the bioactivity of HAp, thus it shouldn't be seen as a negative thing. The sharpness of the phosphate and hydroxyl bands showed the formation of crystalline HAp. Increasing calcination temperatures to 1000 °C increased the sharpness of the PO_4^{3-}(ν1,3) group, which could be attributed to a higher degree of crystallinity (Table 3.2). While the intensity of the OH group's stretching mode decreased with increasing calcination degree, this behaviour could be attributed to the decomposition of HA to β-TCP.

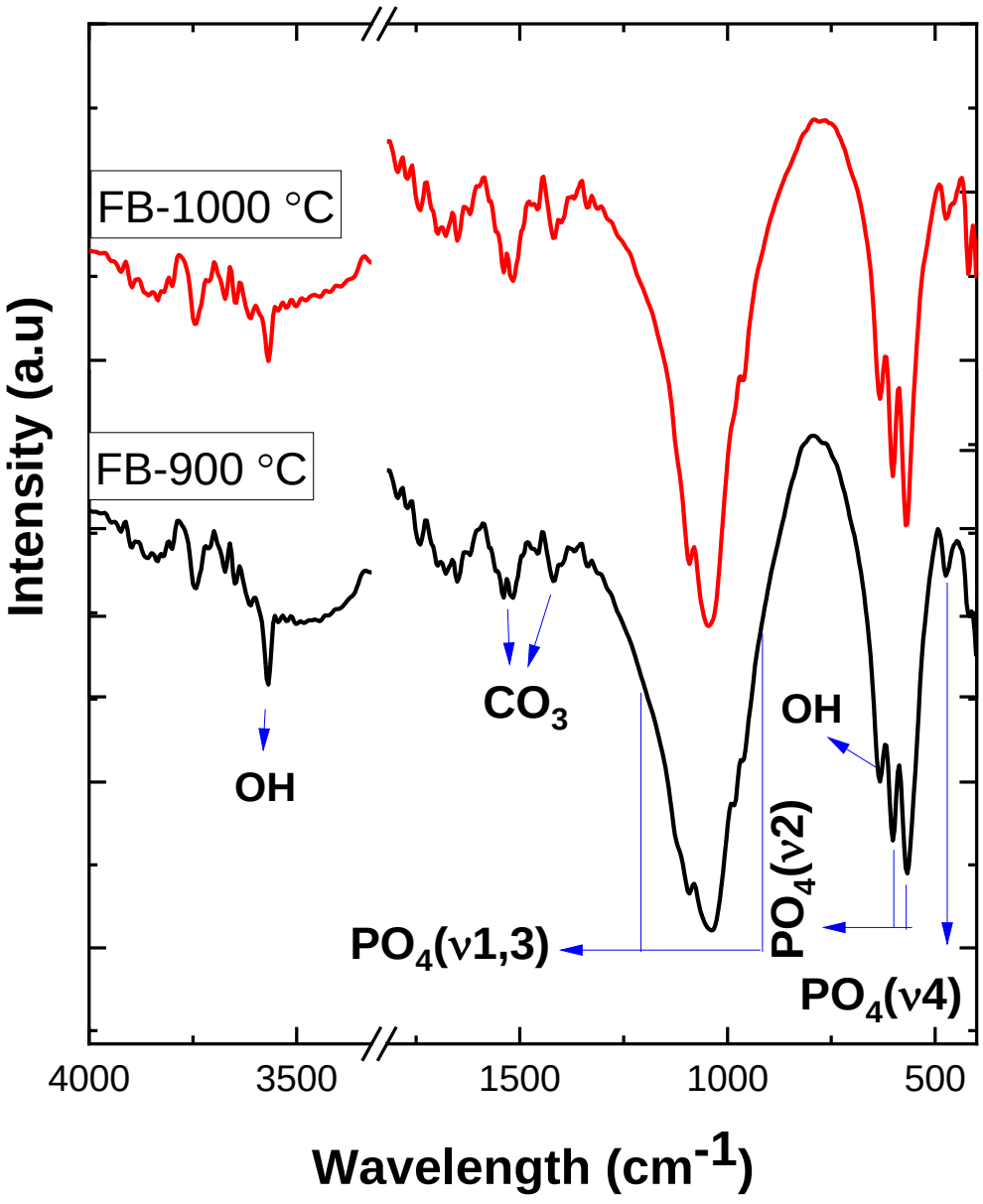

Figure 3.2: FTIR spectra of FB- 900 °C and FB-1000°C materials

3.4 Morphological Analysis

FESEM micrographs of calcined extracted powders at 900 and 1000 °C showed the particles to be irregularly formed agglomerates that were densely packed together (Figure 3-3). During the creation of HAp particles, one or more of the following steps may occur: a) the production of HAp via the processes of nucleation and growth surface free energy is reduced as a consequence of (b) the aggregation of elemental crystals via the molecular attractions of unique scale forces. This causes a decrease in surface-free energy(114). The production of additional crystals inside the aggregates, which occurs under a continuous residual supersaturation, leads to aggregation. After then, this agglomerated particle joins forces with other particles to form secondary particles, which subsequently increase in size(115).

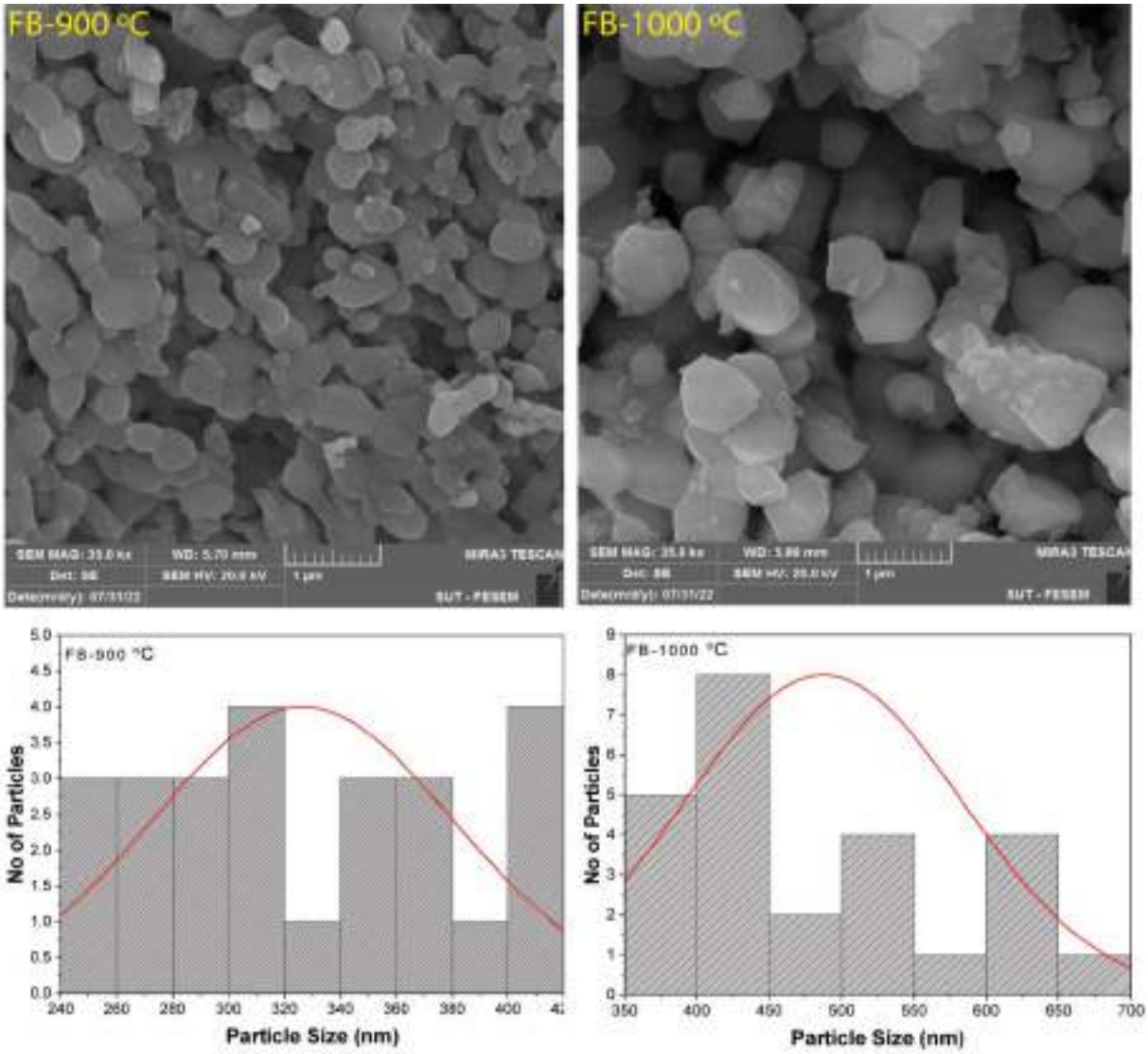

Figure 3.3: FESEM images and Particle-size distribution of FB-900°C and FB-1000°C.

3.5 Calcium-to-phosphorus ratio (Ca/P)

Ca/P atomic ratio of hydroxyapatite (HAp) was determined by Energy Disperse Spectroscopy (EDS). Figure 3.4 shows the most abundant elements in the fish bone were discovered to be calcium and phosphorus. According to the chemical formula of the standard hydroxyapatite, the theoretical calcium to phosphorous molar ratio is approximately 1.67 (76). EDX analysis for the obtained apatite was performed and the results are shown in Fig. 3.4. As shown in the figure, the Ca/P ratio for the apatite obtained by calcination method were 1.68 for FB900 ^{o}C and 1.65 for 1000 ^{o}C, these values lie within the acceptable range for the hydroxyapatite. Variation of these values than the standard HAp value might be due to implication of the carbonate group in the apatites obtained by those methods (79). However, as a new evidence assuring that the apatite obtained by the calcination process being almost free of carbonate, the Ca/P molar ratio of the apatite obtained by such process is very close to the standard one Table 3.3**.**

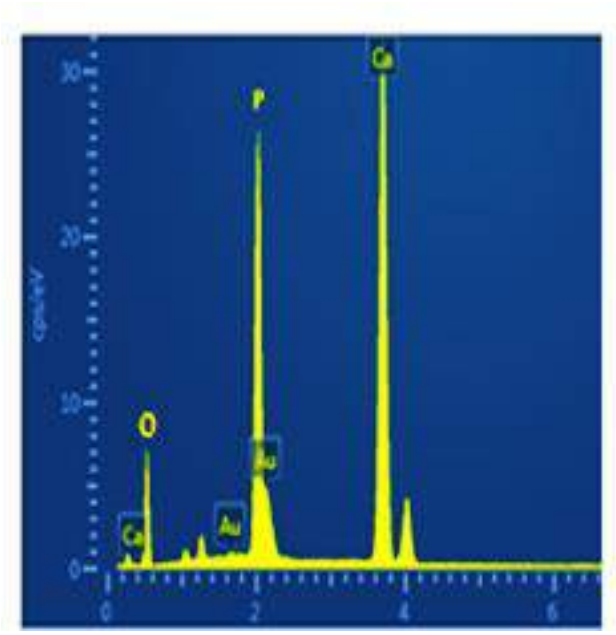

Figure 3.4: EDX images of FB-900°C.

Table 3.3: Comparison of Ca/p ratio of calcined FB at 900 ^{o}C and 1000 ^{o}C

Samples FB	Elemental Composition (wt %)		Ca/P ratio
	Ca	P	
900 ^{O}C	61.12	36.25	1.68
1000 ^{O}C	57.23	34.60	1.65

Elemental mapping was also performed successful of pure phases HAp structure was further confirmed by the homogeneous distribution of Ca, P and O elements in the sample.

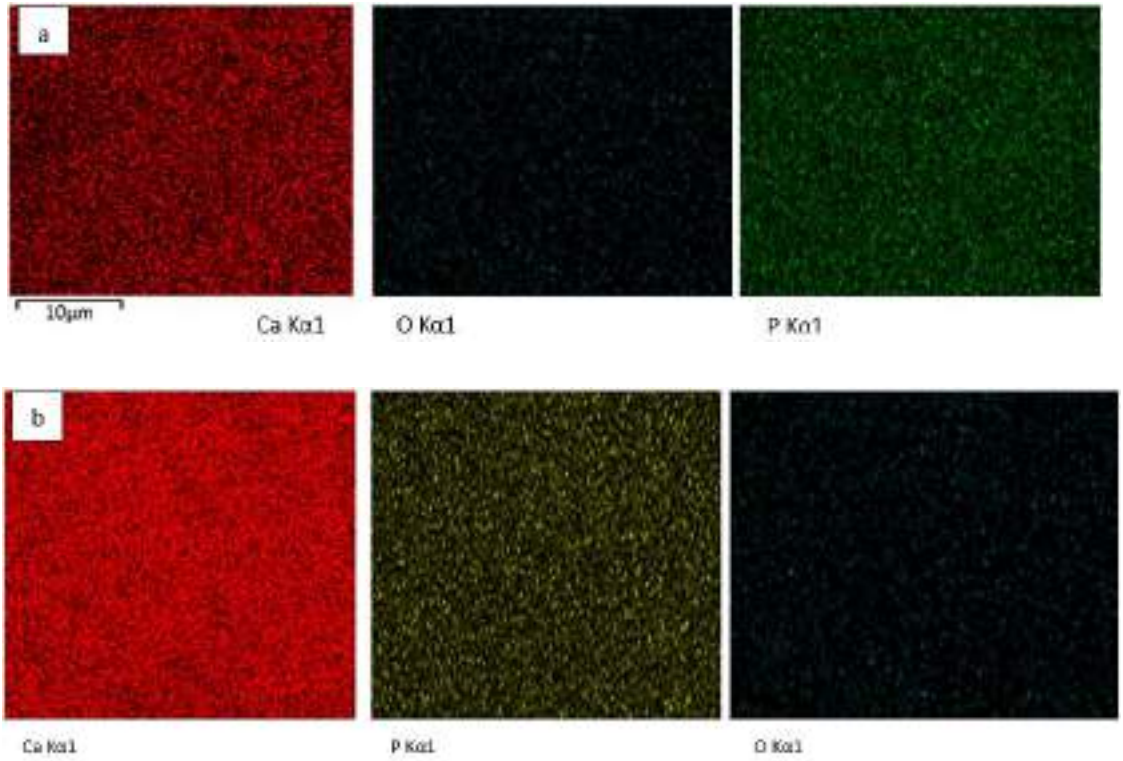

Figure 3.5: Elemental mapping of (a) HA (FB 900), (b) HA (FB 1000)

Table 3.4 shows colour changes (ΔE) RB, HAp-1 and standard hydroxyapatite (HAp-2). The colour characteristic is important which indicates the quality of HAp. Data was stored in L*a*b* colour model and colour changes (ΔE) were calculated with white colour parameter as a reference colour. The result demonstrated that colour changes of HAp-1 at a temperature of 700ºC shows the lowest value (ΔE=17.89) compared to RB and HAp-1 extracted at 600ºC, 800ºC, 900ºC and 1000ºC. This phenomenon may be due to the complete combustion and high degree of purity achieved. This finding is further supported by Venkatesan and Kim (2010), who found that the white colour of the powder indicates the formation of pure HAp. The transition phase of HAp for spotted sardinella (Amblygaster sirm) bone was in the range of 700 to 800°C based on the colour formation. This finding was further supported by Liao et al. (2014) who stated that the transition phase for the formation

of HAp was found at the range of 700 to 850ºC. According to Sofronia et al. (2014) who stated that the optimum temperature for HAp extraction using bovine bone was found at 800ºC. There is a significant difference in colour changes in the value for each temperature for spotted sardinella (Amblygaster sirm) bone. Therefore, calcination temperature at 700ºC is considered as the optimum temperature for HAp extraction in this study. The transition phase of HAp at the optimum temperature was further evaluated, the Ca/P atomic ratio to confirm the formation of HAp.

Table 3.4: Colour changes RB and HAp for fish bone (FB)

Type of sample	Temperature (ºC)	Colour of sample
Raw Bone (RB)	0	Yellowish
Hap	200	Brown
Hap	400	Black
Hap	600	Gray
Hap	800	Off white
Hap	900	White
Hap	1000	Snow white
Standard Hap		White

3.6 Dissolution Behavior

The results of an in vitro dissolution evaluation using SBF that lasted for 14 days and was conducted to determine the dissolution behavior of FB-900°C are shown in Table 3.5 The results provide insight into the possible Ca^{2+} ion concentration present in SBF throughout the course of a period of 14 days. This table demonstrates that the release of Ca^{2+} ions happened quite fast, which signaled the beginning of the pellet's dissolution on its most superficial layers. Ca^{2+} ions concentrations reached their zenith after 24 hours after immersing in SBF, when they were at thei maximum. During the first 24 hours after SBF immersion, the deposition process, on the other hand, emerged as the most important step. The consumption of Ca^{2+} ions may explain

the drop in the concentration of Ca^{2+} ions observed during the development of the apatite layer. Maintaining a constant level of Ca^{2+} concentrations over a period of 7-14 days is evidence that a balance has been struck between the processes of deposition and dissolution.

Table 3.5: Release of Ca^{2+} ion in SBF over 14 days at 37 °C

Immersion time (day)	Release of Ca^{2+} ion (mg/L) in SBF	
	FB-900 °C	**FB-1000** °C
0.0	13.12	12.90
1	23.87	22.88
3	14.79	15.10
7	11.55	10.13
14	9.95	10.07

- STDEV±0.32-0.72

3.7 *In Vitro* Bioactivity

After just one day in the SBF, the surface of each sample exhibited evidence of apatite particle development (Figure 3.6). After a period of one day, increased apatite particle growth was seen. This was attributed to a reduction in sample crystallinity, which made it possible to significantly and quickly release Ca^{2+} ions. After 7 and 14 days in the immersion medium, homogeneous development was observed. The length of time that the sediment was submerged for resulted in an increase in the apatite layer's thickness that had just been produced.

The EDX analysis revealed that the majority of the formed surface particles were composed of calcium, phosphorus, and oxygen, with the Ca and P content steadily decreasing as the immersion period increased. This occurred due to the transformation of the Ca rich-ACP that was initially generated into a layer of stoichiometric crystalline apatite.

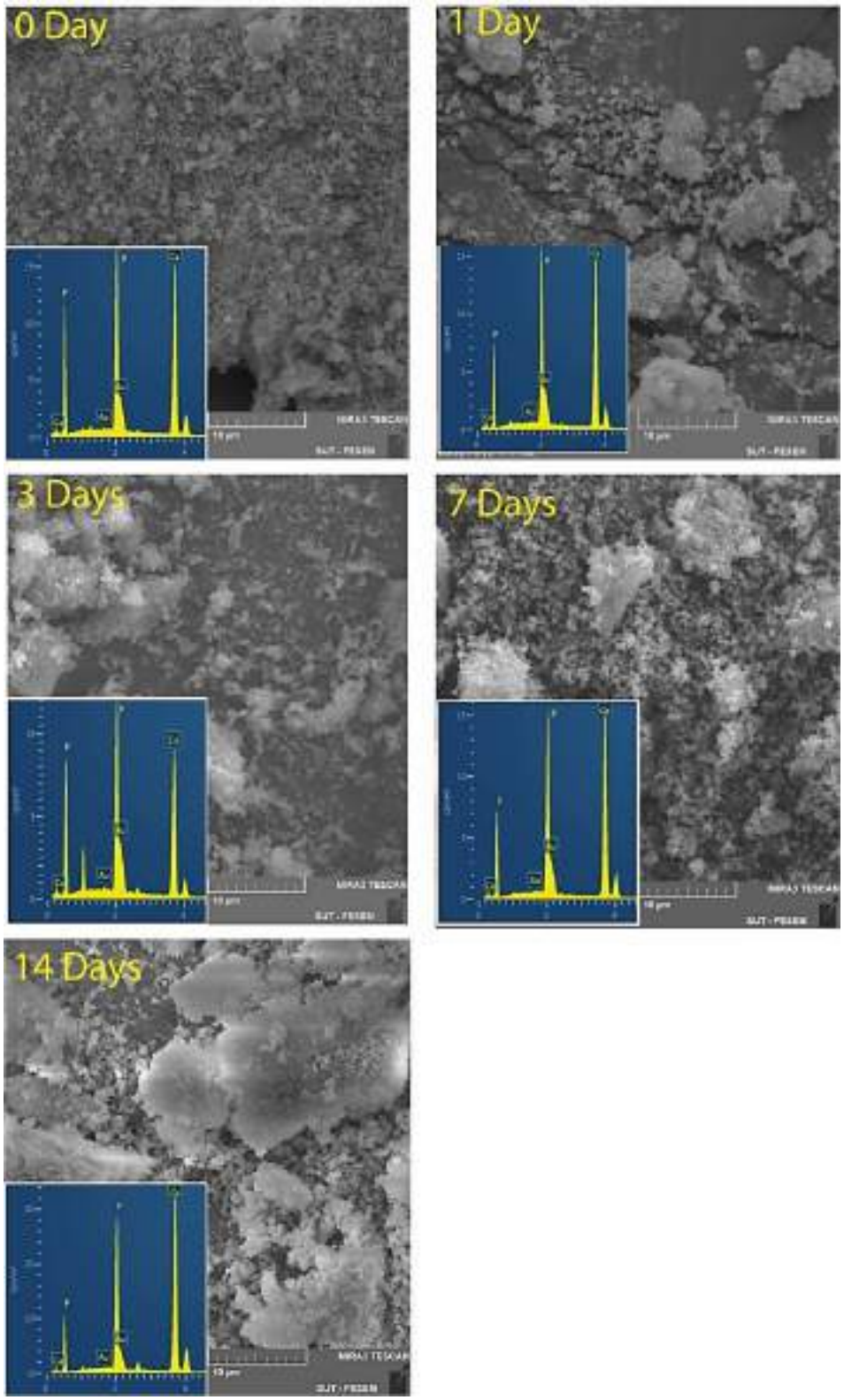

Figure 3.6: FESEM and EDX images of the HA (FB-900°C) after immersion in SBF for 14 days.

3.8. In vitro controlled drug release

3.8.1 In vitro drug release profiles of antibiotics from fish bone (FB 900)

The cumulative release of, amoxicillin, tetracycline and cephalexin from HA is shown in (Figure 3.7). In this study the release profile is seen to be bimodal, where burst release was observed in first 12 h followed by a controlled continuous release. After a fast release of 85 % during the first 12 h, the release rate decreased and cumulative release of 95% cephalexin was observed after 7 days. Whereas 53% burst release of amoxicillin was observed in first 12 h followed by sustained release over 7 days to achieve 75 % release of the loaded drug. The HA containing tetracycline released 48% of the loaded drug after 12 h of immersion, whereas total of 79% loaded drug was released after 7 days. The initial burst release was attributed to the release of drug adsorbed on the outer surface of the samples, while the slow sustained release of the drug was ascribed to the release of drug from within the HA network (116). The burst release in the initial phase followed by a slow release over 7 days is considered favorable to prevent bacterial infection after the surgery. Three possible reasons are suggested for its slow release from HA (i) interaction of organic acid molecules with calcium ions which leads to the formation of antibiotic–calcium phosphate complex (ii) poor water solubility of antibiotic (iii) The change in the nature of loaded matrix, i.e. conversion of the HA reactants into apatite phase. It may result in trapping antibiotic molecules within the apatite crystals (117).

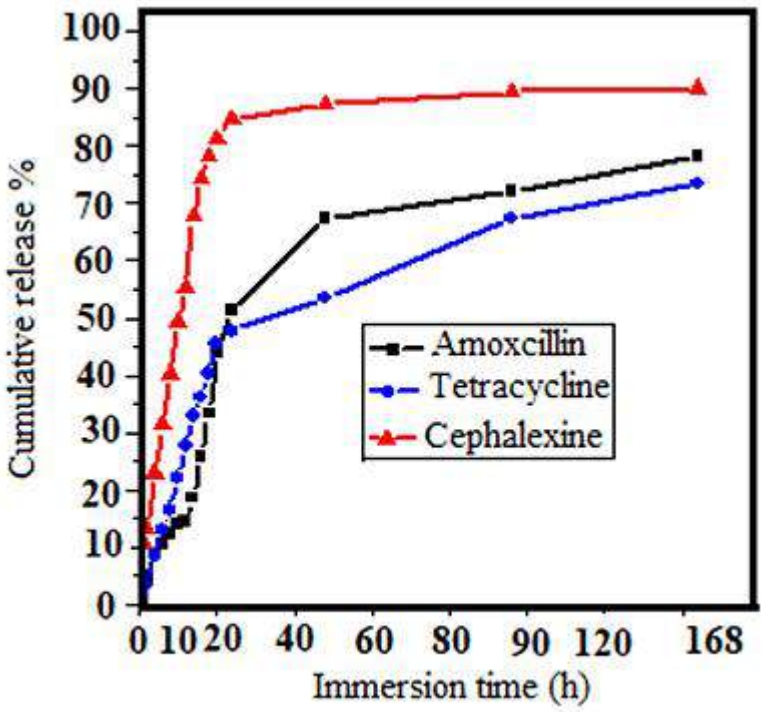

Figure 3.7 *In vitro* release profile of antibiotics from HAp calcined at 900 ^{o}C.

3.9 In vitro antibacterial activity

The antibacterial activity of the cephalexin released from the HAp calcined at 900 ^{o}C was assessed against Escherichia coli (E.coli, ATCC 25922 strains) and Staphylococcus aureus. The samples were incubated with E. coli (ATCC 25922 strains) and Staphylococcus aureus suspension for 24 h. Figure 3.8 exhibits the significant in antibacterial effect. cephalexin incorporated HAp composites inhibited the bacterial growth, as shown in figure 3.8. In this study we have demonstrated that with a cephalexin concentration it should be possible to produce a bone replacement material with antibacterial properties that is likely to inhibit potential post-operative bacterial infections. However, the mechanisms of the anti-bacterial activity are still not fully clear however, previous studies have highlighted three modes of antibacterial activity. (i) in case of any bacterial attack these ions can enter inside the bacterial cells and affect the production of intracellular Adenosine Triphosphate (ATP) and disturb the process of DNA replication, (ii) ions can accumulate in the cell membrane of bacteria and then bring changes in the permeability (the gradual release of proteins and lipopolysaccharides), transportation of protons through the cell membrane is not permitted, which automatically results in the destruction of the cell membrane and the death of the bacterial cell, (iii) induction of reactive oxygen radicals, which can react with the membrane, cell wall of bacteria and mitochondria and ultimately destroy the bacterial cells(118) .

	Staph	E. Coli
Cephalxin	15	20

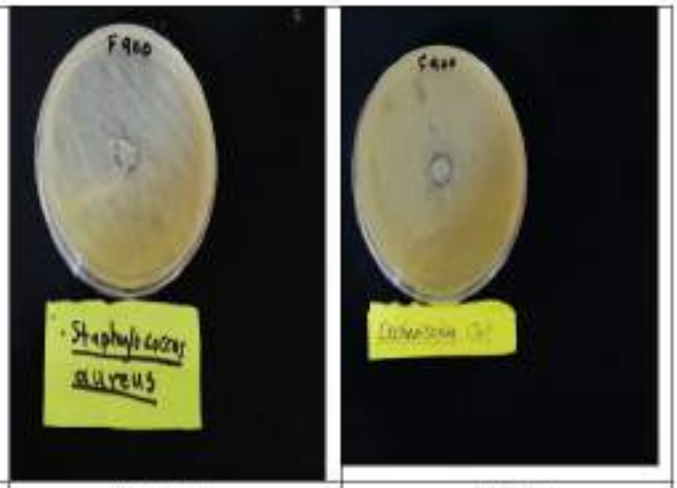

	Stap. aur	E. Coli
F900	13	13

Figure 3.8: Representative photos of E. coli colonies and on FB at 900 ^{o}C

Extraction of Hydroxyapatite (HAp) from chicken legs bone

3.10 X-Ray Diffraction (XRD) Analysis

The dried chicken bones then went through the calcination process in an electric furnace at the temperature of 900, and 1000 °C with a heating rate at 5°C/min for 2 hours.

The phase analysis of HAp powders calcined at 900 °C, and 1000 °C was performed using XRD (Fig3.9). The XRD patterns were validated by comparing it with the HAp standard (ICDD 00-003-0747). At 900 °C and 1000 °C, all the peaks appear were correspond to the standard HAp peaks where the strongest intensity peaks can be found at Miller indices of (002), (210), (211), (300), (202), (310), (222), (213), (304). Thus, it confirms that the XRD analysis of the sample at calcination temperature 900 °C and 1000 °C were in pure HAp phases. The diffraction peaks and lattice parameters were in good agreement with the standard phase of HA (JCDPS 09-432). As the temperature of calcination rising, the crystallinity of the sample also increased as the intensity of the XRD peak has been increased. At 900 °C, the major peaks show a form of HAp. However, minor peaks belong to beta tri-calcium phosphate (β-TCP) starting to emerge at this temperature. This is owing to the HAp decomposition, which above a certain temperature, HAp started to decomposes, allowing β-TCP to produce. According to some research, HAp begins to decompose to β-TCP at a temperature(119).

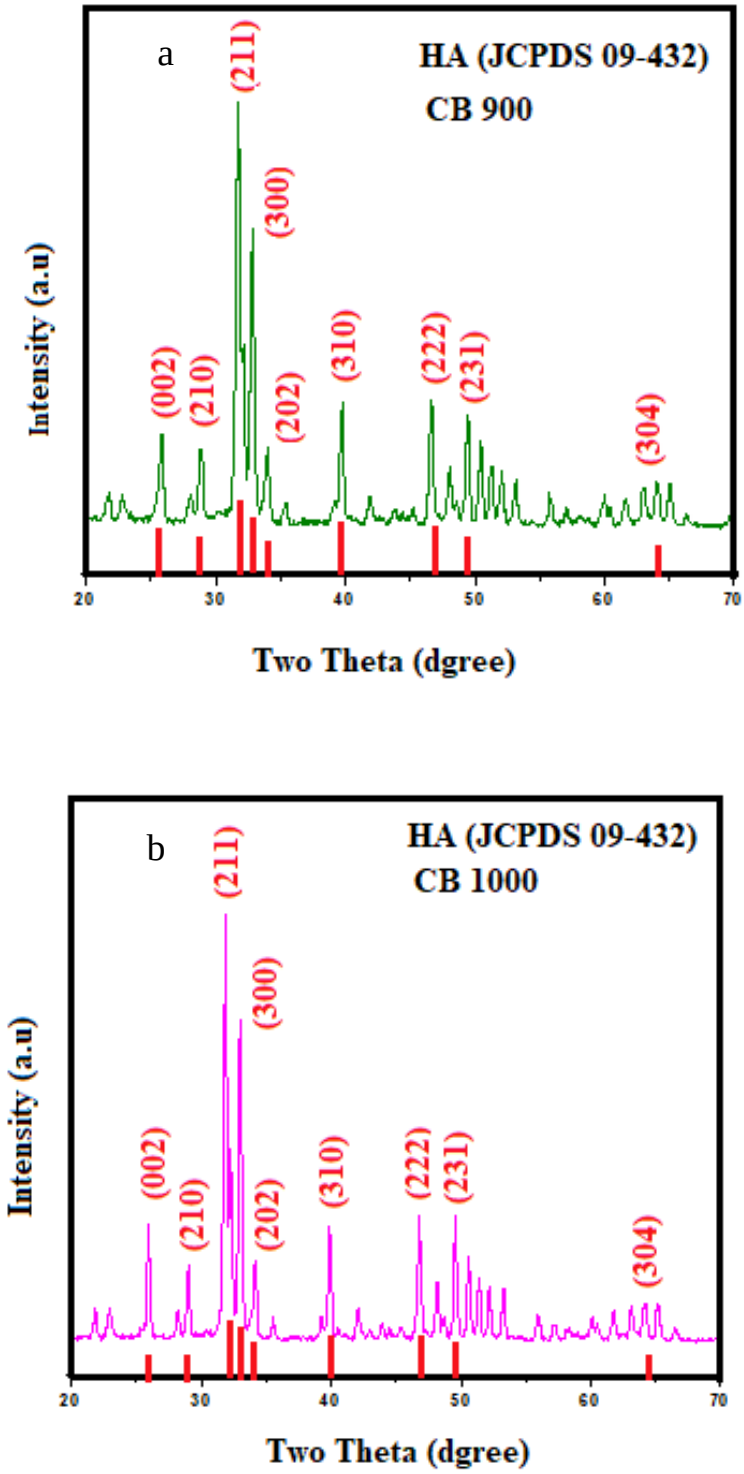

Figure 3.9: XRD pattern of HA calcined at (a) CB 900) and (b) CB1000°C for 2 h

Table 3.6: Lattice parameters of HA from chicken bone (CB) calcined at 900 ̊C and 000 ̊C plus degree of crystallinity.

Samples	Chemical formula	Lattice Parameter			X_c	*D*
	$Ca_{10}(PO_4)_6(OH)_2$	*a* (Å)	*c* (Å)	*V* (Å)^3	(%)	(nm)
Standard HA	$Ca_5(PO_4)_3(OH)$	9.418	6.884	528.8	----	----
HA (900)	$Ca_{10}(PO_4)_6(OH)_2$	9.419	6.873	527.5	86	97.22
HA (1000)	$Ca_{10}(PO_4)_6(OH)_2$	9.416	6.866	527.3	84	96.35

Table 3.7: Peak List

Pos. [°2Th.]	FWHM Left [°2Th.]	d-spacing [Å]	Rel. Int. [%]
10.856370	0.196800	8.14961	12.29
21.802440	0.196800	4.07652	11.56
22.946520	0.295200	3.87580	8.71
25.937420	0.246000	3.43526	22.66
27.989560	0.344400	3.18788	8.57
28.987290	0.147600	3.08039	22.28
31.786250	0.196800	2.81524	100.00
32.938520	0.246000	2.71935	77.35
34.103150	0.196800	2.62910	22.38
34.544620	0.196800	2.59650	7.23
39.897090	0.246000	2.25965	27.82
42.062330	0.246000	2.14820	8.33
43.894960	0.295200	2.06267	4.88
45.287090	0.590400	2.00245	3.18
46.695430	0.295200	1.94529	24.78
48.096640	0.295200	1.89184	12.02
49.598540	0.295200	1.83801	22.63
50.607270	0.295200	1.80372	19.14
51.385460	0.246000	1.77822	14.25
52.202980	0.295200	1.75228	12.53
53.225520	0.295200	1.72100	11.97
55.992050	0.295200	1.64235	5.77
57.178990	0.295200	1.61105	4.16
60.120740	0.344400	1.53907	7.00
61.756020	0.344400	1.50218	6.62
63.144400	0.295200	1.47245	9.88
64.146380	0.393600	1.45185	9.79
65.145810	0.344400	1.43198	10.94
66.564470	0.393600	1.40486	2.90
71.777830	0.295200	1.31511	5.39

3.11 FT-IR analysis

Figure 3.10 demonstrates the FTIR spectra of chicken bone calcinated bone at different temperatures (900°C, and 1000°C). As shown in Figure 4.2, the spectra of chicken bone and heated ones are obviously different due to the changes in their chemical bonds during heat treatment. Through visual observation, the color of bone particles changes from yellowish white to white after calcination. Through FTIR spectra, it is also revealed the presence of phosphate (PO_4^{3-}), and hydroxyl (OH^-) groups. These spectra are more clearly appeared in calcinated samples because the calcination process has destroyed the cross-linked structure in the chicken bone. Four vibrational modes of the phosphate (PO_4^{3-}) group were recorded at 520 cm^{-1} (PO_4^{3-} (ν2), 480 cm^{-1} (PO_4^{3-} (ν2), 530 cm^{-1} (PO_4^{3-} (ν4), and 980-1200 cm^{-1} (PO_4^{3-} (ν1,3). The stretching and bending mode of hydroxyl (OH) group were observed at 3566 cm^{-1} and 634 cm^{-1} The sharp narrow band at wide band at 3572 cm^{-1} are associated with hydroxyl group where these peaks prove the presence of HAP phase.

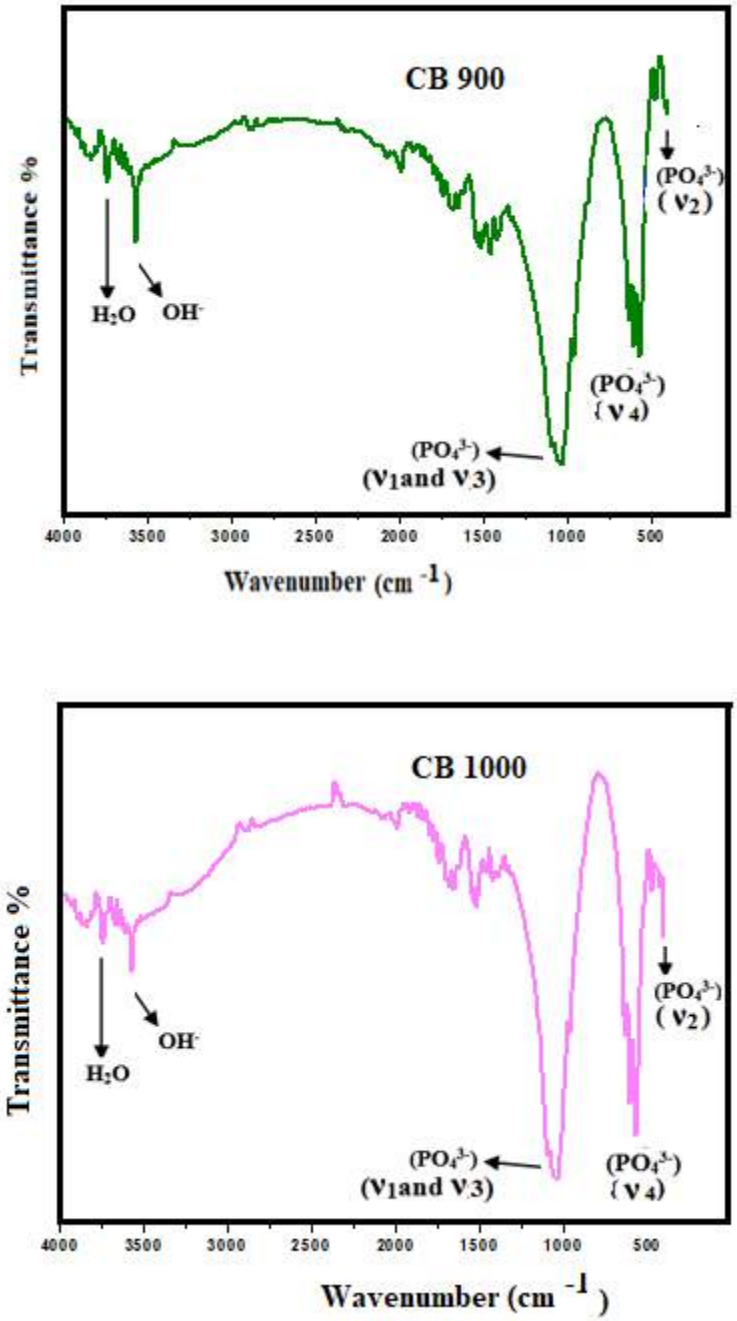

Figure 3.10: FTIR Spectra of HAP powder Calcined at (a) CB 900) and (b) CB1000°C for 2 h

3.12 FESEM Analysis

The morphology of the extracted HAp from chicken bone was observed using FESEM. The FESEM micrograph in Fig. 3.11 shows that the HAp powder has an irregular shape for all calcination temperatures (900 °C, and 1000 °C). At the temperature of 900 °C, the presence of an uneven irregular-shaped HAp can be seen. The particle sizes of powder were ranging from 300 to 530 nm. As the temperature of calcination increase, the size of HAp structures begins to increase and it was further increased until temperature 1000 °C. The FESEM micrograph in Fig. 3.11 shows that the HAp particles tended to agglomerate as the temperature increased. In addition, Venkatesan et al. suggested that the complete removal of organic moieties by calcination method results in the particles growing (120). Thus, it supports the result shows in Fig. 3.11 that as the temperature increase, the size of the particle also increases.

The HAp exhibited larger particle size with spherical shape. The increase of calcination temperature influenced the grain growth and crystallization of HAp particle due to the absorption of heat energy during chemical synthesis process. Fewer pores can be observed in the sample

The increasing time makes HAp to have tiny volume and their surface-to-volume ratios were much larger. However, these high surface areas were accompanied by Van der Waals interaction that can create a strong tendency to agglomerate. The particle size, shape and surface roughness have effect on the properties of the particles. The particle size plays an important role in the drug release profile of the particles. Moreover, the morphology of HAP particles also depends on the source of the bone, holding time and temperature of calcination.

The particles become finer as the calcination temperature increases. It might also be influenced by the gender, age, and food habit of the animals from which the bone was collected. Hence, more studies are required to understand the influence of these biological factors on the morphology. However, a calcination temperature of 900°C has proven to be the best temperature for the isolation of the best quality HAp from both CB.

3.13 Calcium-to-phosphorus ratio (Ca/P)

Ca/P ratio of hydroxyapatite (HAp) was determined by Energy Disperse Spectroscopy (EDS). Figure 3.11. shows the most abundant elements in the fish bone were discovered to be calcium and phosphorus. According to the chemical formula of the standard hydroxyapatite, the theoretical calcium to phosphorous molar ratio is approximately 1.67. EDX analysis for the obtained apatite was performed and the results are shown in Fig. 3.12. As shown in the Table 4.3, the Ca/P ratio for the apatite obtained by the subcritical water and alkaline hydrothermal methods were 1.66 and 1.63 foe 900 and 1000 ^{o}C respectively these values lie within the acceptable range for the hydroxyapatite. Variation of these values than the standard HAp value might be due to implication of the carbonate group in the apatites obtained by those methods. However, as a new evidence assuring that the apatite obtained by the calcination process being almost free of carbonate, the Ca/P molar ratio of the apatite obtained by such process is very close to the standard. Elemental mapping was also performed successful of pure phases-HAp structure was further confirmed by the homogeneous distribution of Ca, P and O elements in the sample Figure 4.5.

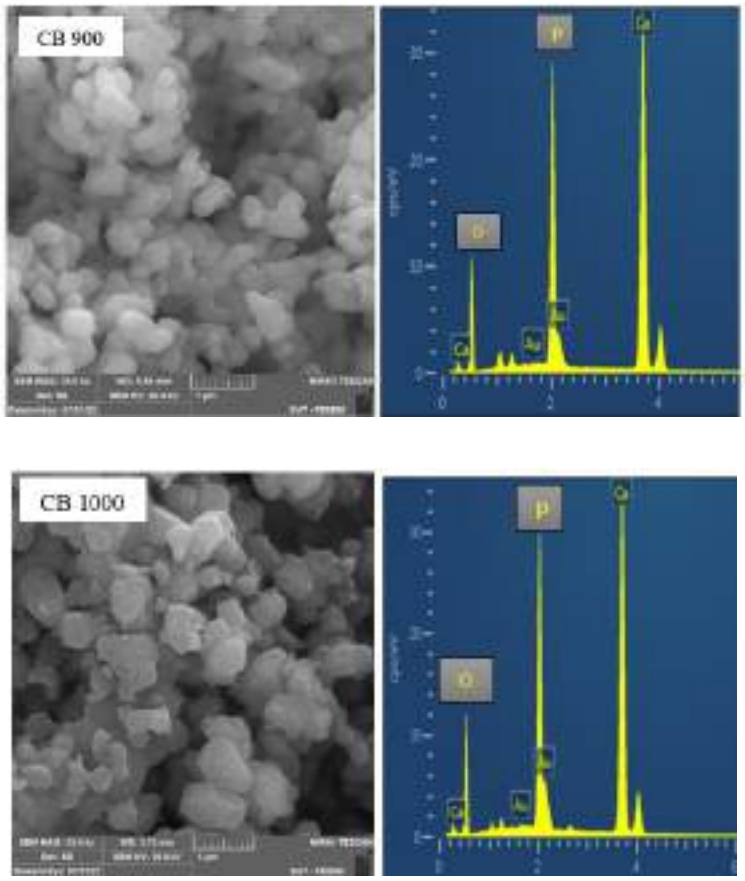

Figure 3.11: FESEM and EDX images showing the morphology of (a) HA (CB 900 °C), (b) HA (CB 1000 °C).

able 3.8: Comparison of Ca/p ratio of calcined CB at 900 °C and 1000 °C

Samples CB	Elemental Compostion (wt %)		Ca/P ratio
	Ca	P	
900 °C	62.33	37.38	1.66
1000 °C	57.35	35.14	1.63

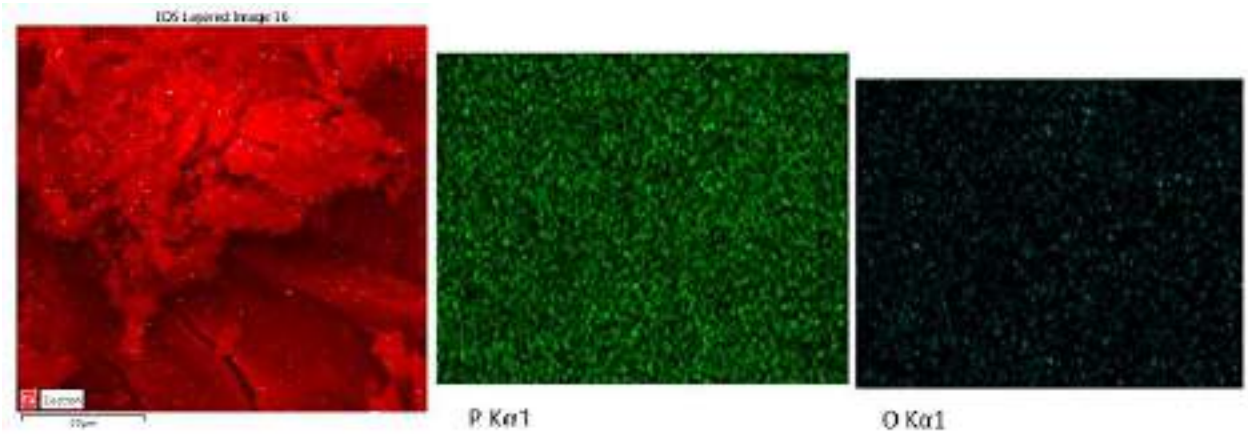

Figure 3.12: Elemental mapping of (a) HA (CB 900), (b) HA (CB 1000)

In this study, HA was extracted from bovine cortical bone by multi stage annealed at different temperature sequentially. About 65% HA was extracted from this process, similar to reported studies (Bahrololoomaet al., 2009). During annealed at different temperature, the percentage of weight loss and color change of bovine bone are shown in Table 3.9. After annealing at different temperatures, the color of the bone was changed due to removal of organic portion. The color of the raw bovine bone was observed as yellowish white, which was consequently altered into yellow, light yellow, black and gray at 200°C, 250°C, 500°C and 650°C temperatures respectively. The color of the bovine bone was turned into white with further increase in the temperature. The different colorwas observed below 800°C, revealed the association of the organic matrix within the bone. Therefore, it can be inferred that about ~35 % of total weight loss was due to removal of water and organic substance from the bovine bone when annealed up to about 850°C.

Table 3.9: Colour changes RB and HAp for chicken bone (CB)

Type of sample	Temperature (ºC)	Colour of sample
Raw Bone (RB)	0	Light yellow
Hap	200	Light brown
Hap	400	Black
Hap	600	Gray
Hap	800	Off white
Hap	900	White
Hap	1000	Snow white
Standard Hap		White

3.14 Dissolution Behavior

Table 3.10 Shows the release of Ca^{2+} ions in SBF over 14 days, it was noted that the Ca^{2+} ion concentration in SBF began to increase immediately, indicating the initiation of the surface level dissolution of the pellet. Highest Ca^{2+} concentration in SBF was recorded after 24 h of immersion in SBF. However, the concentration of Ca^{2+} ion began to decline due to the consumption of Ca^{2+} ions in the formation of the apatite layer, indicating that the deposition process was the dominant process after the first 24 h of the immersion in SBF. The concentration of Ca^{2+} was fairly stable between 7 to 14 days hence indicating that the equilibrium between the deposition and dissolution has been attained.

Table 3.10: Release of Ca^{2+} ion in SBF over 14 days at 37 ˚C

Immersion time (day)	Release of Ca^{2+} ion (mg/L) in SBF	
	HA (FB900)	HA (FB1000)
0.0	13.17	12.90
1	22.75	20.58
3	16.66	15.10
7	12.57	11.13
14	10.78	10.07

SD± 0.32-0.72

3.15 In Vitro Bioactivity

Growth of apatite particle was observed on the surface of all samples (Figure 3.13) just after 1 day of immersion in SBF. The degree of growth of apatite particles increased 1d in which was attributed to the reduced degree of crystallinity of samples leading to the faster and higher release of Ca^{2+} ions (Figure 3.13). After 7 and 14 days of immersion, homogeneous growth was observed. This newly formed apatite layer grew in intensity over prolonged immersion time.

EDX analysis confirmed that the particles formed on the surface were predominantly composed of Ca, P and O with The Ca, P steadily decreased with increase in immersion time which was due to the transformation of initially formed Ca rich-ACP into stoichiometric crystalline apatite layer.

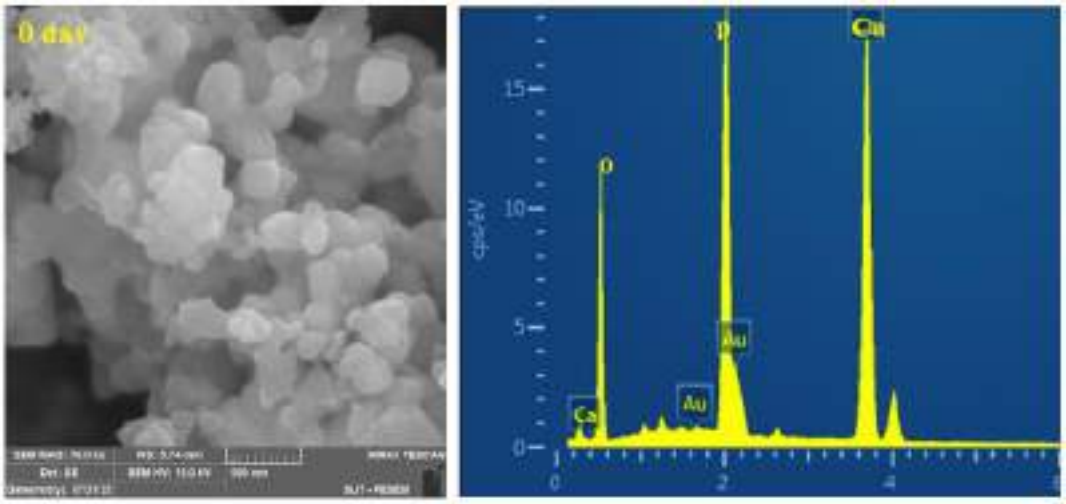
0 day
P
Cu
O
Au
Au
Co
cps/eV
15
10
5
0
0
2
4

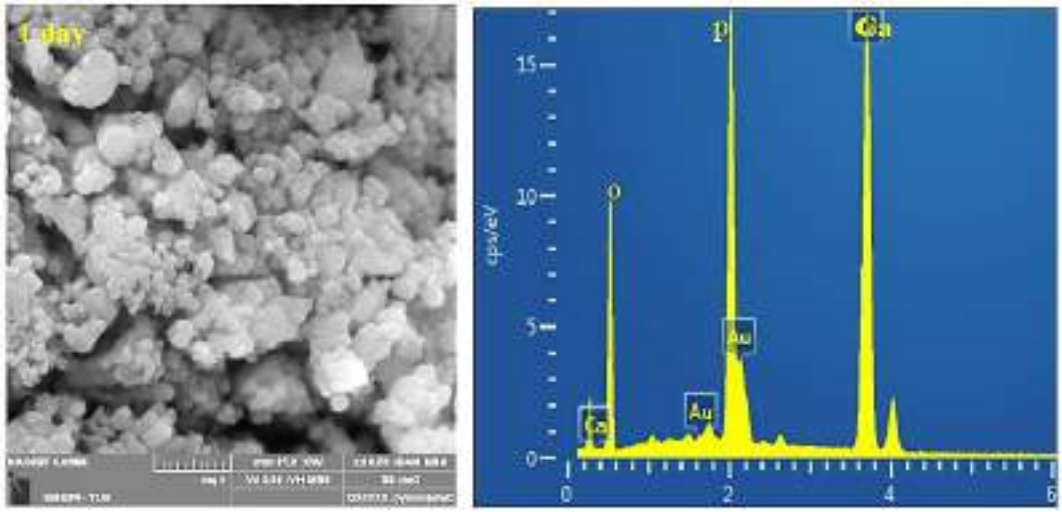
1 day
P
Ga
O
Au
Au
Co
cps/eV
15
10
5
0
0
2
4
6

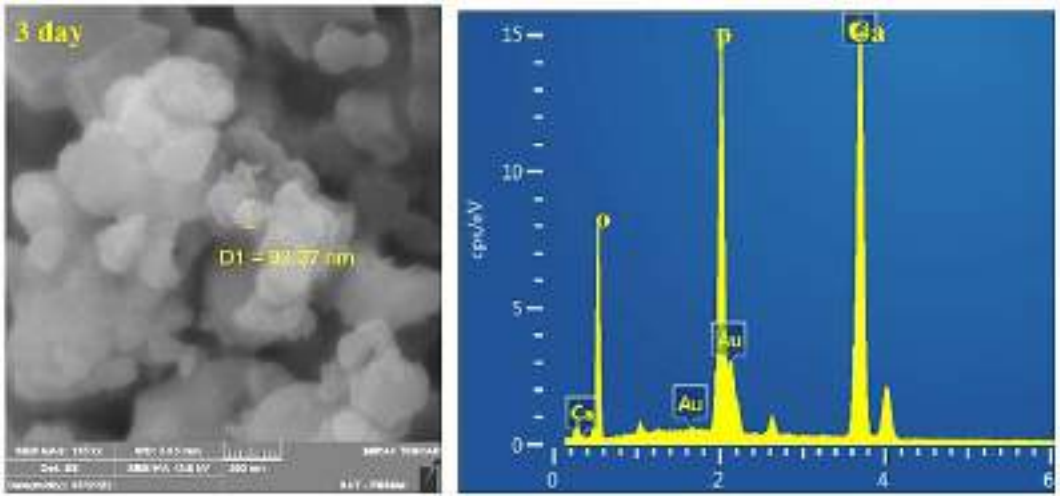
3 day
D1 = 98.37 nm
P
Ga
O
Au
Au
Co
cps/eV
15
10
5
0
0
2
4
6

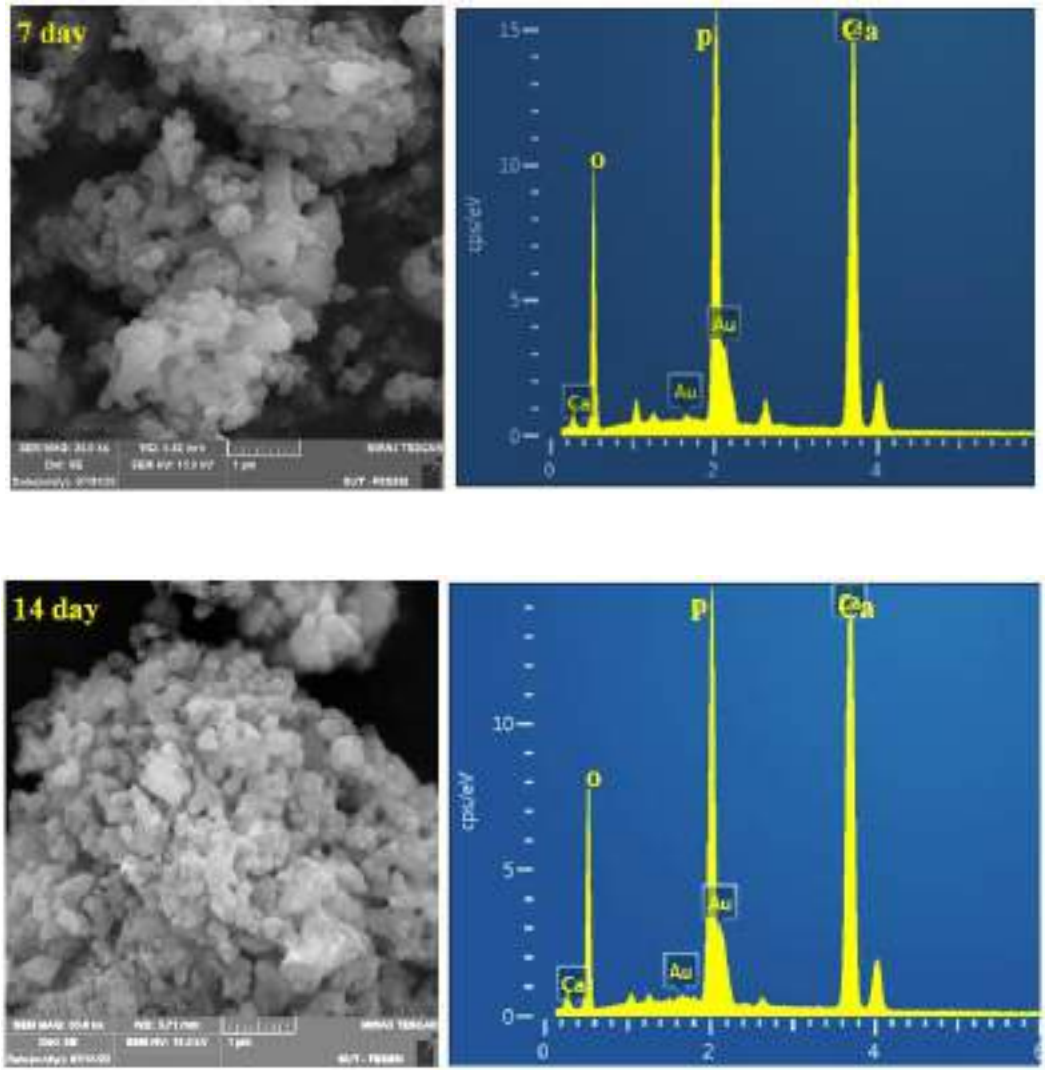

Figure 3.13: FESEM and EDX images of the HA (CB 900) after immersion in SBF over 14 days.

In vitro controlled drug release

3.16 In vitro drug release profiles of antibiotics from chicken bone (CB 900 ^{o}C)

The cumulative release of, amoxicillin, tetracycline and cephalexin from HA is shown in (Figure 3.14). In this study the release profile is seen to be bimodal, where burst release was observed in first 12 h followed by a controlled continuous release. After a fast release of 80 % during the first 12 h, the release rate decreased and cumulative release of 96.3% cephalexin was observed after 14 days. Whereas 65% burst release of tetracycline was observed in first 12 h followed by sustained release over 14 days to achieve 86 % release of the loaded drug. The HAp containing amoxicillin released 45% of the loaded drug after 12 h of immersion, whereas total of 75% loaded drug was released after 14 days. The initial burst release was attributed to the release of drug adsorbed on the outer surface of the samples, while the slow sustained release of the drug was ascribed to the release of drug from within the HAp network. The burst release in the initial phase followed by a slow release over 14 days is considered favorable to prevent bacterial infection after the surgery. Three possible reasons are suggested for its slow release from cement (i) interaction of organic acid molecules with calcium ions which leads to the formation of antibiotic–calcium phosphate complex (ii) poor water solubility of antibiotic (iii) The change in the nature of loaded matrix, i.e. conversion of the cement reactants into apatite phase. It may result in trapping antibiotic molecules within the apatite crystals.

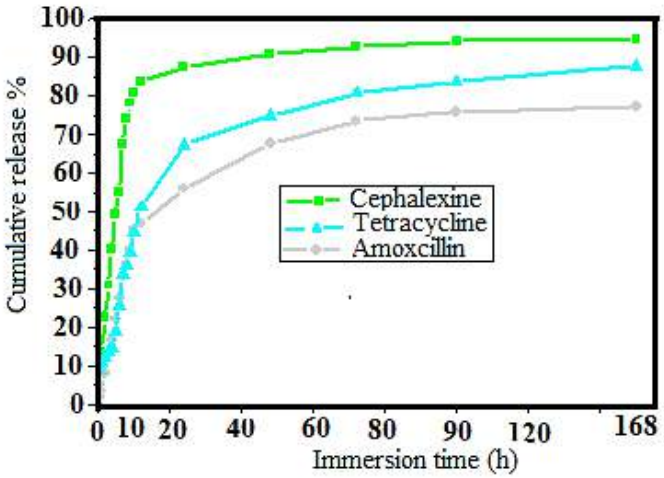

Figure 3.14: *In vitro* drug release profiles of antibiotics from chicken bone (CB 900)

3.17 In vitro antibacterial activity

Biomaterials for medical applications should be evaluated with in vitro investigations of antimicro bial properties before clinical trials (Alt et al., 2004). The antimicrobial activity of the synthe sized hydroxyapatite was assessed by the well diffusion assay against human pathogenic strains in clouding yeast, Gram-positive and Gram-negative bacteria. (Figure 3.15).

The antibacterial activity of the HAp loaded antibiotic released was assessed against the *Escherichia coli* (*E.coli*, ATCC 25922 strains) and *Staphylococcus aureus*. The samples were incubated with *E. coli* (ATCC 25922 strains) and *Staphylococcus* aureus suspension for 24 h. Figure 3.15 exhibits the significant in antibacterial effect. In this study we have demonstrated that with a cephalexin concentration it should be possible to produce a bone replacement material with antibacterial properties that is likely to inhibit potential post-operative bacterial infections.

	Staph	E. Coli
CB 900	15	14

Figure 3.15: Representative photos of *E. coli* and *Staphylococcus aureus* colonies on CB at 900 ^{o}C

Extraction of Hydroxyapatite (HAp) from sheep legs bone (SB)

3.18 X-Ray Diffraction (XRD) Analysis

The structural analysis of the sheep legs bone (SB) powder heated in different temperatures was done by XRD (figure.3.16). The phase analysis of size controlled HAp is compared with the ICCD (International Centre for Diffraction Data standard HAp) PDF card no. 00-009-0432 which shows that the major diffraction peaks at 2θ values of 26.801, 28.601 32.026°, 33.424°, 34.165°, 40.722° 46.954°, and 52.271° corresponding to the (002), (210), (211), (300), (202), and (310),(222) and (213) Miller planes are in good agreement with the standard HAp. This result of XRD analysis obtained in the present investigation is in good agreement with the reported results.

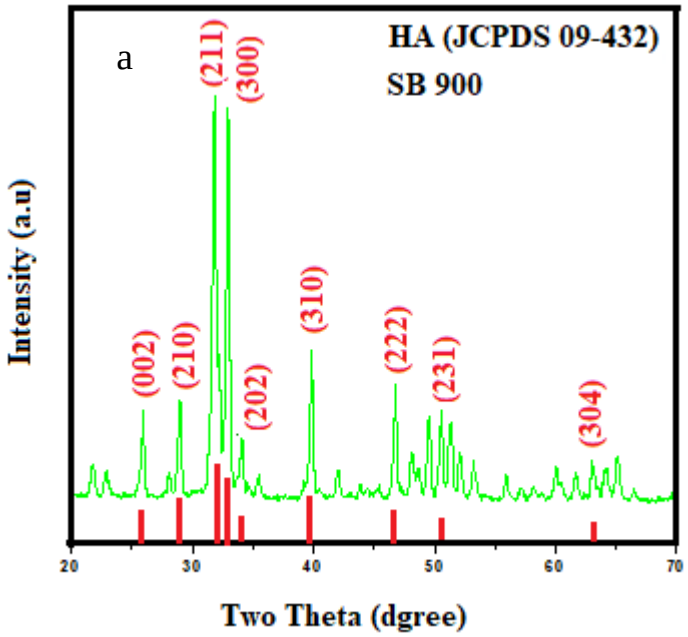

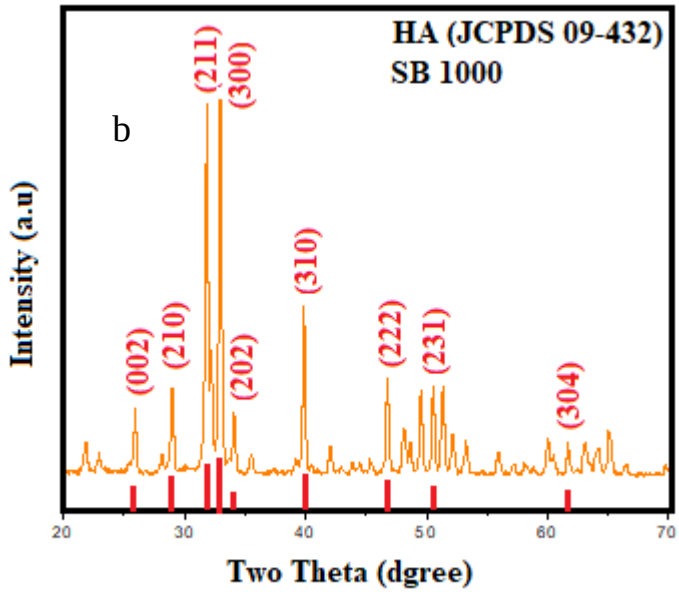

Figure 3.16: XRD pattern of HA calcined at (a) SB 900 and (b) SB1000°C for 2 h.

Table 3.11: Lattice parameters of HA from sheep bone (SB) calcined at 900 and 1000 ^{o}C plus degree of crystallinity.

Samples	Chemical formula	Lattice Parameter			X_c	*D*
	$Ca_{10}(PO_4)_6(OH)_2$	*a* (Å)	*c* (Å)	*V* (Å)^3	(%)	(nm)
Standard HA	$Ca_5(PO_4)_3(OH)$	9.418	6.884	528.8	----	----
HA (900)	$Ca_{10}(PO_4)_6(OH)_2$	9.418	6.866	527.4	86	98.23
HA (1000)	$Ca_{10}(PO_4)_6(OH)_2$	9.415	6.858	527.2	85	98.28

Table 3.12: Peak List

Pos. [°2Th.]	FWHM Left [°2Th.]	d-spacing [Å]	Rel. Int. [%]
21.826210	0.246000	4.07214	7.22
25.824510	0.344400	3.45002	25.95
28.845880	0.295200	3.09517	21.70
31.648840	0.295200	2.82715	100.00
32.835950	0.295200	2.72761	83.75
34.016450	0.196800	2.63560	23.24
35.406550	0.246000	2.53525	6.55
39.798350	0.344400	2.26502	27.13
41.950020	0.295200	2.15369	8.38
44.442950	1.180800	2.03850	2.22
46.730480	0.344400	1.94391	27.49
47.998660	0.246000	1.89547	14.10
49.494450	0.393600	1.84163	28.57
50.508900	0.442800	1.80700	21.45
51.298330	0.344400	1.78103	16.48
52.088780	0.295200	1.75585	13.04
53.136990	0.344400	1.72366	11.94
55.869530	0.295200	1.64566	6.69
57.072280	0.393600	1.61381	4.23
60.102890	0.787200	1.53948	5.71
61.629550	0.393600	1.50496	7.39
63.057040	0.344400	1.47428	10.67
64.204380	0.541200	1.45068	9.71
65.051310	0.344400	1.43383	11.72
71.680420	0.393600	1.31666	6.04

3.19 FTIR reults

FTIR spectra analysis in the range of 4000 to 400 cm^{-1} was employed to characterize the different functional groups present in the bone powder of hydroxyapatite.

The FTIR spectrum also revealed all characteristic absorption peaks of hydroxyapatite, showing the presence of phosphate (PO_4^{3-}), hydroxyl (OH^-). The first indication of hydroxyapatite is in the form of a strong band at about 609 and 1040 cm^{-1}, which is associated with the presence of a phosphate group (PO_4^{3-}). The results of these FTIR analyses show that heating sheep legs bone (SB) powder at 900 and 1000 °C for 2 h will produce a calcium phosphate compound with characteristic hydroxyapatite phase. Figure 3.17 depicted the FTIR spectra of synthesized HAP powder at 2 different calcination temperature (2 hours). It can be observed that the FTIR spectrum contained a functional group of phosphate at bands 1084, 520 and 480 cm^{-1}. The hydroxyl group (OH^-) was identified at 3390 and 627 cm^{-1}. The presence of water also can be found at 3390 cm^{-1}. OH^- group also existed at 640 cm^{-1} and water molecules at 3078 and 3585 cm^{-1}. The absorption peaks that appeared around 1400-1600 cm^{-1} indicated carbonate ion substitution.

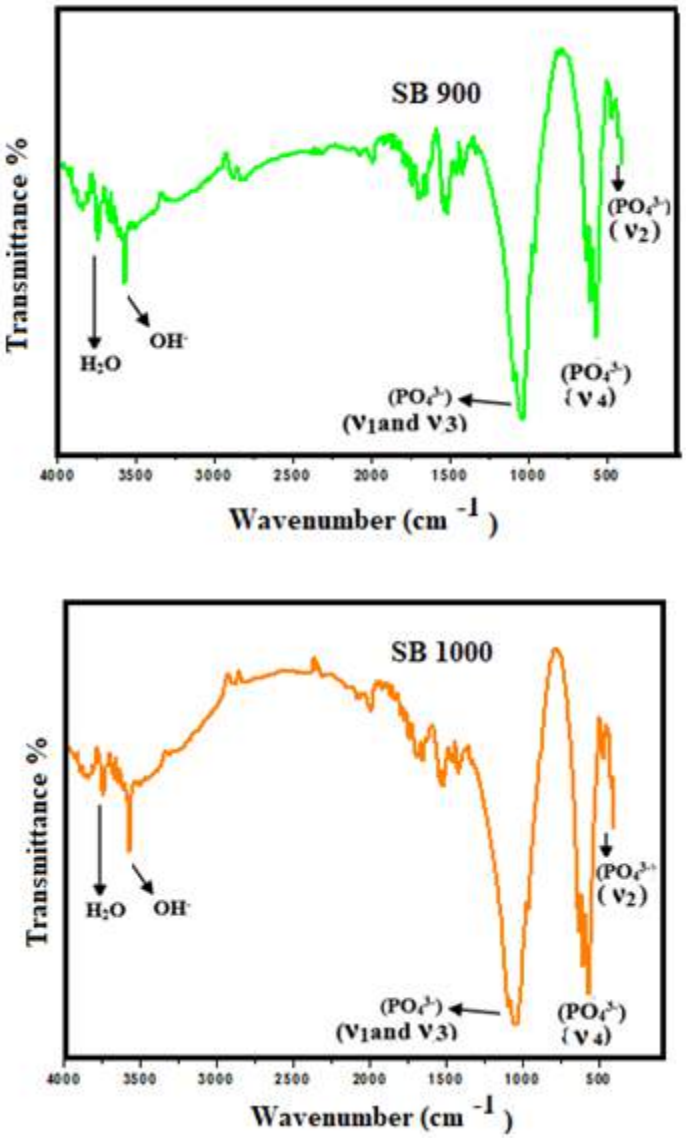

Figure 3.17: FTIR Spectra of HAP powder Calcined of (a) SB 900 and (b) SB1000°C for 2 h.

3.20 FESEM Analysis

FSEM analysis indicated that the obtained powders are composed of rod-like shape particles with submicron average size. Their microstructural characteristics, the bones annealed at 900 and 1000 °C were observed by FSEM (Fig. 3.18). Two clearly different grain structures can be observed in the micrograph: smaller rounded ones, and much larger and more crystalline looking ones, with a more elongated shape. The latter form needle-like crystals around 500 nm wide and several microns long, and they tend to orient together with the longer axis aligned in the same direction. These features confirm that two different phases are present in the material.

3.21 Calcium-to-phosphorus ratio (Ca/P)

Table 3.13 show the elemental analysis from EDS enables for the Ca/P ratio to be calculated. At 900 °C, the ratio of Ca/P obtained was 1.65, and owing to the presence of these trace elements. However, as the temperature of calcination increased to 1000 °C, the ratio of Ca/P was 1.62 and the closest to the HAp theoretical ratio which is 1.67. At the calcination phase of 900 °C – 1000 °C, monophase of HAp started to maintain and this phase resulting in a close ratio of Ca/P. Elemental mapping was also performed successful of pure phases- HAp structure was further confirmed by the homogeneous distribution of Ca, P and O elements in the sample Figure 3.19

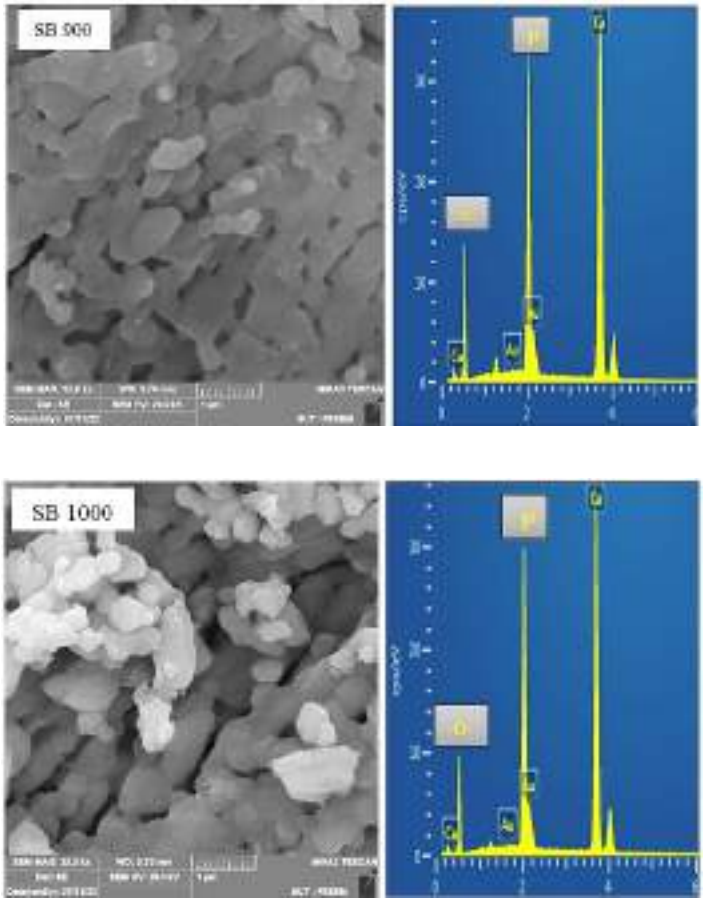

Figure 3.18: FESEM and EDX images showing the morphology of (a) HAp (SB 900 °C), (b) HAp (SB 1000 °C).

Table 3.13: Comparison of Ca/p ratio of calcined SB at 900 °C and 1000 °C

Samples SB	Elemental Compostion (wt%)		Ca/P ratio
	Ca	P	
900 °C	60.05	36.31	1.65
1000 °C	55.32	34.10	1.62

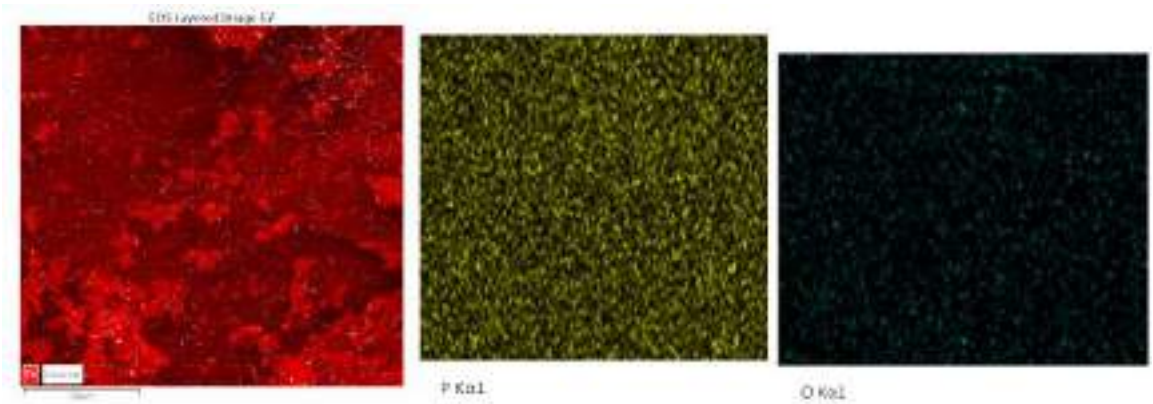

Figure 3.19: Elemental mapping of (a) HA (SB 900), (b) HA (SB 1000)

different temperatures, the color of the bone was changed due to removal of organic portion. The color of the raw bovine bone was observed as yellowish white, which was consequently altered into yellow, light yellow, black and gray at 200°C, 250°C, 500°C and 650°C temperatures respectively. The color of the bovine bone was turned into white with further increase in the temperature. The different color was observed below 800°C, revealed the association of the organic matrix within the bone. Therefore, it can be inferred that about ~35 % of total weight loss was due to removal of water and organic substance from the bovine bone when annealed up to about 850°C.

Table 3.14: Colour changes RB and HAp for sheep bone (SB)

Type of sample	Temperature (ºC)	Colour of sample
Raw Bone (RB)	0	Yellowish
Hap	200	Light brown
Hap	400	Dark brown
Hap	600	Black
Hap	800	Off white
Hap	900	White
Hap	1000	Snow white
Standard Hap		White

3.22 Dissolution Behavior

Table 3.15 Shows the release of Ca^{2+} ions in SBF over 14 days, it was noted that the Ca^{2+} ion concentration in SBF began to increase immediately, indicating the initiation of the surface level dissolution of the pellet. Highest Ca^{2+} concentration in SBF was recorded after 24 h of immersion in SBF. However, the concentration of Ca^{2+} ion began to decline due to the consumption of Ca^{2+} ions in the formation of the apatite layer, indicating that the deposition process was the dominant process after the first 24 h of the immersion in SBF. The concentration of Ca^{2+} was fairly stable between 7 to 14 days hence indicating that the equilibrium between the deposition and dissolution has been attained.

Table 3.15: Release of Ca^{2+} ion in SBF over 14 days at 37 ˚C

Immersion time (day)	Release of Ca^{2+} ion (mg/L) in SBF	
	HA (SB 900)	HA (SB 1000)
0.0	14.10	13.90
1	24.45	21.88
3	13.79	14.10
7	10.55	10.13
14	8.95	9.07

SD± 0.32-0.72

3.23 In Vitro Bioactivity

Growth of apatite particle was observed on the surface of all samples (Figure 3.20) just after 1 day of immersion in SBF. The degree of growth of apatite particles increased 1d in which was attributed to the reduced degree of crystallinity of samples leading to the faster and higher release of Ca^{2+} ions (Figure 3.20). After 7 and 14 days of immersion, homogeneous growth was observed. This newly formed apatite layer grew in intensity over prolonged immersion time.

EDX analysis confirmed that the particles formed on the surface were predominantly composed of Ca, P and O with The Ca, P steadily decreased with increase in immersion time which was due to the transformation of initially formed Ca rich-ACP into stoichiometric crystalline apatite layer.

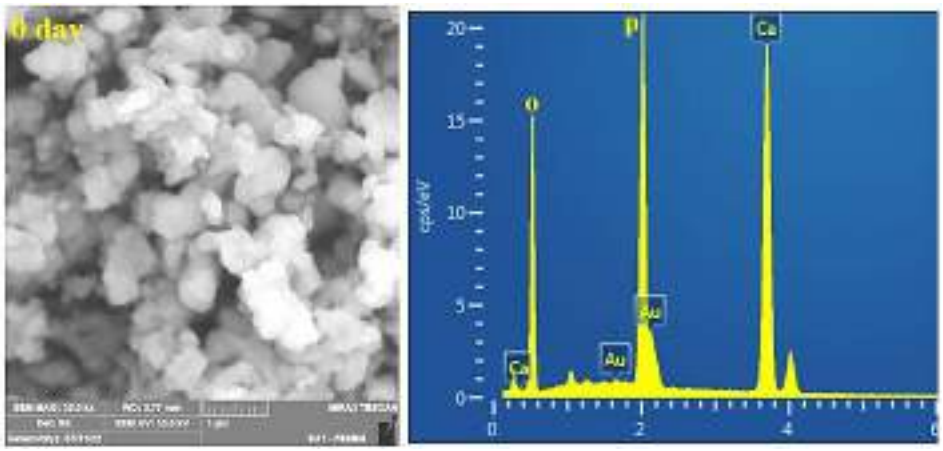
0 day
cps/eV
O
P
Ca
Au
Au
Ca

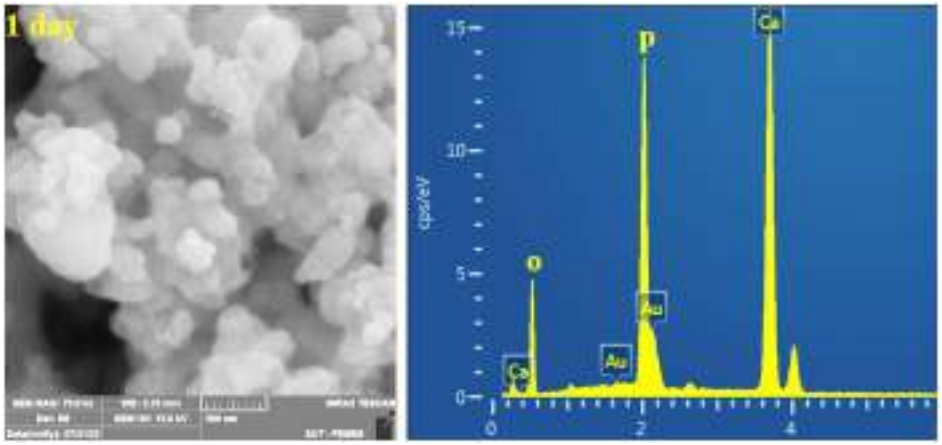
1 day
cps/eV
O
P
Ca
Au
Au
Ca

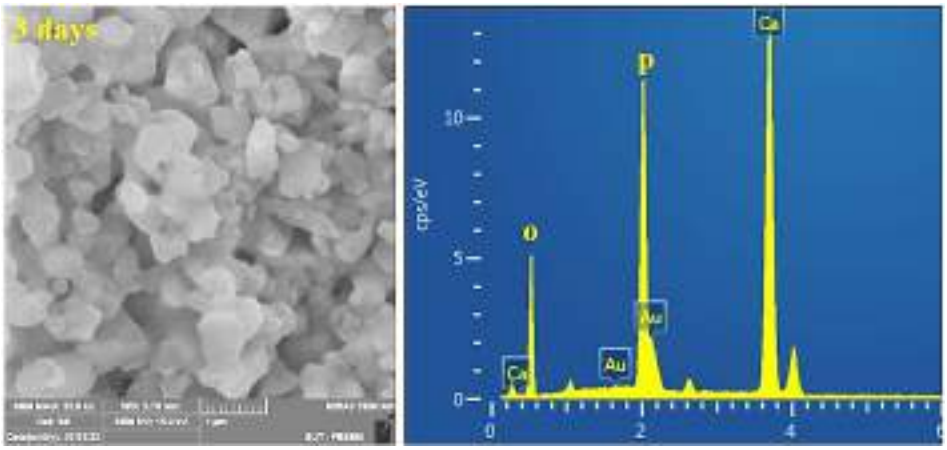
3 days
cps/eV
O
P
Ca
Au
Au
Ca

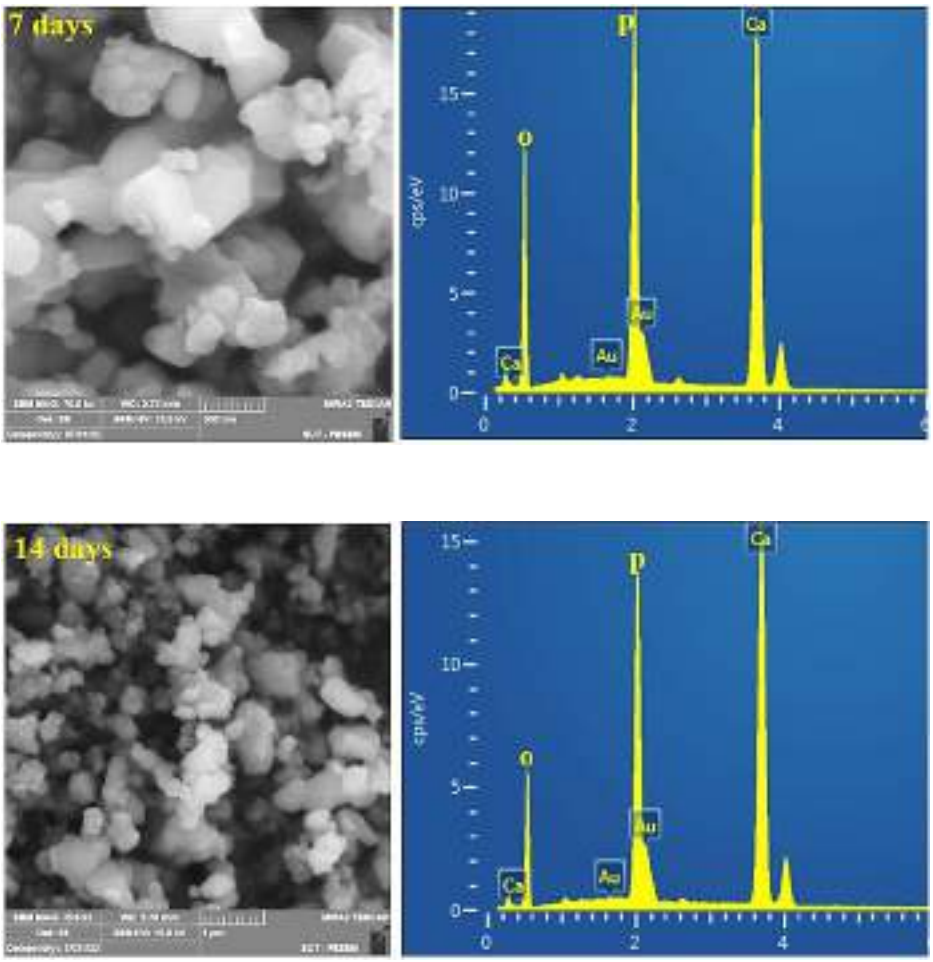

Figure 3.20: FESEM and EDX images of the HA (SB 900) after immersion in SBF over 14 days

3.24 In vitro drug release profiles of antibiotics from sheep bone (SB 900)

The cumulative release of cephalexin, amoxicillin and tetracycline from HAp is shown in (Figure 3.21).In this study the release profile is seen to be bimodal, where burst release was observed in first 12 h followed by a controlled continuous release. After a fast release of 65 % during the first 12 h, the release rate decreased and cumulative release of 75.4% cephalexin was observed after 14 days. Whereas 47% burst release of amoxicillin was observed in first 12 h followed by sustained release over 14 days to achieve 68 % release of the loaded drug. The HAp containing tetracycline released 68% of the loaded drug after 12 h of immersion, whereas total of 78% loaded drug was released after 14 days. The initial burst release was attributed to the release of drug adsorbed on the outer surface of the samples, while the slow sustained release of the drug was ascribed to the release of drug from within the cement network. The burst release in the initial phase followed by a slow release over 14 days is considered favorable to prevent bacterial infection after the surgery. Three possible reasons are suggested for its slow release from cement (i) interaction of organic acid molecules with calcium ions which leads to the formation of antibiotic–calcium phosphate complex (ii) poor water solubility of antibiotic (iii) The change in the nature of loaded matrix, i.e. conversion of the cement reactants into apatite phase. It may result in trapping antibiotic molecules within the apatite crystals.

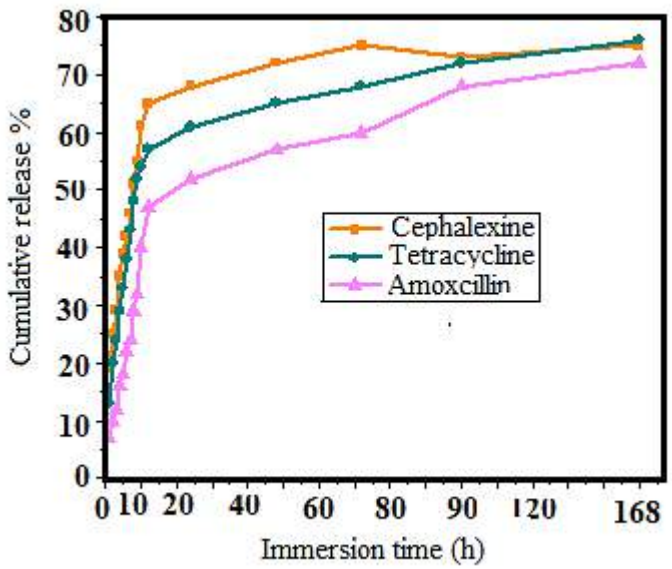

Figure 3.21: In vitro drug release profiles of antibiotics from sheep bone (SB 900 ^{o}C)

3.25 In vitro antibacterial activity

In this study we have demonstrated that with a change in antibiotic concentration it should be possible to produce a bone replacement material with antibacterial properties that is likely to inhibit potential post-operative bacterial infections. The antimicrobial activity of the synthe sized hydroxyapatite was assessed by the well diffusion assay against human pathogenic strains in clouding yeast, Gram-positive and Gram-negative bacteria. (Figure 3.22).

The antibacterial activity of the HAp loaded antibiotic released was assessed against the Escherichia coli (E.coli, ATCC 25922 strains) and Staphylococcus aureus. The samples were incubated with E. coli (ATCC 25922 strains) and Staphylococcus aureus suspension for 24 h. Figure 4.6 exhibits the significant in antibacterial effect. In this study we have demonstrated that with a cephalexin concentration it should be possible to produce a bone replacement material with antibacterial properties that is likely to inhibit potential post-operative bacterial infections

	Staph	E. Coli
SB 900	15	14

Figure 3.22: Representative photos of E. coli colonies and on FB at 900 ^{o}C

CONCLUSIONS AND RECOMMENDATIONS

Conclusions

The HAp was extracted from fish bone, chicken bone and sheep bone by calcination method and characterized by FT-IR spectrophotometer, XRD, FESEM and EDX (attached with FESEM), obtain pure phase of synthesized HAp. We have successfully employed calcination method to extracted phase pure HAp with Ca/P molar ratio of 1.68. These releases of antibiotic provided substantial antimicrobial activity, which demonstrates good properties of these materials.

The key factors for the success of surgical interventions aimed at the implantation of prosthesis or osteoconductive materials are the prevention from postoperative bacterial infections. Incorporation of antimicrobial agents such as antibiotics or other antimicrobial agents in DCP cements can prevent post-surgical infections. HAp demonstrated excellent antibacterial against E-coli.

The cumulative release of gentamicin sulphate, amoxicillin and ampicillin trihydrate from brushite cement systems was investigated. In this study the release profile is seen to be bimodal, where burst release is observed in first 12 h followed by a controlled continuous release. The initial burst release is attributed to the release of drug adsorbed on the outer surface of the samples, while the slow sustained release of the drug is ascribed to the release of drug from within the cement network. The burst release in the initial phase followed by a slow release over 7 days is considered favorable to prevent bacterial infection after the surgery.

Recommendations

1. The HAp was extracted from fish bone, chicken bone and sheep bone by calcination method. Therefore, they are potential candidates for various orthopaedic and dental applications. However, their ultimate use as a biomaterial is subject to good in-vivo biocompatibility and low cytotoxicity.
2. Therefore, study to establish osteoblast cells proliferation and their ability to mineralize the bone matrix should be conducted to establish suitability of these materials as useable biomaterials. Infections are not always produced by the same bacteria; therefore, it would be of importance to propose a system that could be combined with many different drugs, in such a way that the surgeon could choose the drug just before implantation.
3. Various drugs have different effects on HAp properties, and this represents a serious drawback for the implementation of this technology. A lot of work is required to establish the general laws that control the release profile of these types of materials, in order to be able to adjust them to different therapeutically needs and to obtain reproducible and predictable drug delivery systems.

REFERENCES

References

1. Hertel R. Fractures of the proximal humerus in osteoporotic bone. Osteoporosis International. 2005;16:S65-S72.
2. Razfar N, Reeves JM, Langohr DG, Willing R, Athwal GS, Johnson JA. Comparison of proximal humeral bone stresses between stemless, short stem, and standard stem length: a finite element analysis. Journal of shoulder and elbow surgery. 2016;25(7):1076-83.
3. Kumar A, Gori Y, Yadav B, Rana S, Sharma NK. FEA of humerus bone fracture and healing. Advanced Materials for Biomechanical Applications: CRC Press; 2022. p. 255-72.
4. Nandi SK, Roy S, Mukherjee P, Kundu B, De DK, Basu D. Orthopaedic applications of bone graft & graft substitutes: a review. Indian Journal of Medical Reseach. 2010;132(1):15-30.
5. Schumaier A, Grawe B. Proximal humerus fractures: evaluation and management in the elderly patient. Geriatric Orthopaedic Surgery & Rehabilitation. 2018;9:2151458517750516.
6. Pu'ad NASM, Koshy P, Abdullah HZ, Idris MI, Lee TC. Syntheses of hydroxyapatite from natural sources. Heliyon. 2019;5(5):e01588.
7. Lertcumfu N, Jaita P, Manotham S, Jarupoom P, Eitssayeam S, Pengpat K, et al. Properties of calcium phosphates ceramic composites derived from natural materials. Ceramics International. 2016;42(9):10638-44.
8. O'Hare P, Meenan BJ, Burke GA, Byrne G, Dowling D, Hunt JA. Biological responses to hydroxyapatite surfaces deposited via a co-incident microblasting technique. Biomaterials. 2010;31(3):515-22.
9. Boskey AL. Third Edit. Elsevier; 2013.
10. Mour M, Das D, Winkler T, Hoenig E, Mielke G, Morlock MM, et al. Advances in porous biomaterials for dental and orthopaedic applications. Materials. 2010;3(5):2947-74.
11. Feng C, Xue J, Yu X, Zhai D, Lin R, Zhang M, et al. Co-inspired hydroxyapatite-based scaffolds for vascularized bone regeneration. Acta Biomaterialia. 2021;119:419-31.
12. Zhang D, Wu X, Chen J, Lin K. The development of collagen based composite scaffolds for bone regeneration. Bioactive materials. 2018;3(1):129-38.
13. Falconer JL, Grainger DW. 1.4 Silver antimicrobial biomaterials. Compr Biomater II. 2017;1:79-91.
14. Adzila S, Murad M, Sopyan I. Doping metal into calcium phosphate phase for better performance of bone implant materials. Recent Patents on Materials Science. 2012;5(1):18-47.

15. Dhandayuthapani B, Sakthi kumar D. Biomaterials for biomedical applications. Biomedical Applications of Polymeric Materials and Composites. 2016:1-20.
16. Engstrand J, Persson C, Engqvist H. The effect of composition on mechanical properties of brushite cements. Journal of the mechanical behavior of biomedical materials. 2014;29:81-90.
17. Dorozhkin SV. Calcium orthophosphate cements for biomedical application. Journal of Materials Science. 2008;43(9):3028-57.
18. Rollo JMDdA, Boffa RS, Cesar R, Schwab DC, Leivas TP. Assessment of trabecular bones microarchitectures and crystal structure of hydroxyapatite in bone osteoporosis with application of the Rietveld method. Procedia Engineering. 2015;110:8-14.
19. Bhat SV. Biomaterials: Alpha Science Int'l Ltd.; 2005.
20. Sofronia AM, Baies R, Anghel EM, Marinescu CA, Tanasescu S. Thermal and structural characterization of synthetic and natural nanocrystalline hydroxyapatite. Materials Science and Engineering: C. 2014;43:153-63.
21. Hoffman RM. Patient-derived orthotopic xenografts: better mimic of metastasis than subcutaneous xenografts. Nature Reviews Cancer. 2015;15(8):451-2.
22. Habraken W, Habibovic P, Epple M, Bohner M. Calcium phosphates in biomedical applications: materials for the future? Materials Today. 2016;19(2):69-87.
23. Mohd Pu'ad NAS, Koshy P, Abdullah HZ, Idris MI, Lee TC. Syntheses of hydroxyapatite from natural sources. Heliyon. 2019;5(5):e01588.
24. De Groot K. Bioceramics Calcium Phosphate: CRC press; 2018.
25. Al-Haddad A, Che Ab Aziz ZA. Bioceramic-based root canal sealers: a review. International journal of biomaterials. 2016;2016.
26. Moradi A, Pakizeh M, Ghassemi T. A review on bovine hydroxyapatite; extraction and characterization. Biomedical Physics & Engineering Express. 2022;8(1):012001.
27. Yelten-Yilmaz A, Yilmaz S. Wet chemical precipitation synthesis of hydroxyapatite (HA) powders. Ceramics International. 2018;44(8):9703-10.
28. Terzioğlu P, Öğüt H, Kalemtaş A. Natural calcium phosphates from fish bones and their potential biomedical applications. Materials Science and Engineering: C. 2018;91:899-911.
29. Zakaria SM, Sharif Zein SH, Othman MR, Yang F, Jansen JA. Nanophase hydroxyapatite as a biomaterial in advanced hard tissue engineering: a review. Tissue Engineering Part B: Reviews. 2013;19(5):431-41.

30. Piccirillo C, Pullar RC, Costa E, Santos-Silva A, Pintado MME, Castro PML. Hydroxyapatite-based materials of marine origin: A bioactivity and sintering study. Materials Science and Engineering: C. 2015;51:309-15.
31. Ni Z, Gu X, He Y, Wang Z, Zou X, Zhao Y, et al. Synthesis of silver nanoparticle-decorated hydroxyapatite (HA@ Ag) poriferous nanocomposites and the study of their antibacterial activities. RSC advances. 2018;8(73):41722-30.
32. Bahrololoom ME, Javidi M, Javadpour S, Ma J. Characterisation of natural hydroxyapatite extracted from bovine cortical bone ash. J Ceram Process Res. 2009;10(2):129-38.
33. Sallemi I, Ayed FB, Bouaziz J, editors. Effect of fluorapatite additive on the mechanical properties of tricalcium phosphate-zirconia composites2012: IOP Publishing.
34. Yokoi T, Goto T, Kato T, Takahashi S, Nakamura J, Sekino T, et al. Hydroxyapatite formation from octacalcium phosphate and its related compounds: a discussion of the transformation mechanism. Bulletin of the Chemical Society of Japan. 2020;93(5):701-7.
35. Lawton DM, Lamaletie MDJ, Gardner DL. Biocompatibility of hydroxyapatite ceramic: response of chondrocytes in a test system using low temperature scanning electron microscopy. Journal of Dentistry. 1989;17(1):21-7.
36. Pramanik N, Mishra D, Banerjee I, Maiti TK, Bhargava P, Pramanik P. Chemical synthesis, characterization, and biocompatibility study of hydroxyapatite/chitosan phosphate nanocomposite for bone tissue engineering applications. International journal of biomaterials. 2009;2009.
37. Do Prado Ribeiro DC, de Abreu Figueira L, Mardegan Issa JP, Dias Vecina CA, JosÉDias F, Da Cunha MR. Study of the osteoconductive capacity of hydroxyapatite implanted into the femur of ovariectomized rats. Microscopy research and technique. 2012;75(2):133-7.
38. Jaramillo CD, Rivera JA, Echavarría A, O'Byrne J, Congote D, Restrepo LF. Osteoconductive and osseointegration properties of a commercial hydroxyapatite compared to a synthetic product. Revista Colombiana de Ciencias Pecuarias. 2010;23(4):471-83.
39. Jang HL, Lee HK, Jin K, Ahn H-Y, Lee H-E, Nam KT. Phase transformation from hydroxyapatite to the secondary bone mineral, whitlockite. Journal of materials chemistry B. 2015;3(7):1342-9.
40. Brown WE, Chow LC. Chemical properties of bone mineral. Annual Review of Materials Science. 1976;6(1):213-36.
41. Ayatollahi MR, Yahya MY, Asgharzadeh Shirazi H, Hassan SA. Mechanical and tribological properties of hydroxyapatite nanoparticles extracted from natural bovine bone and the bone cement developed by nano-sized bovine hydroxyapatite filler. Ceramics International. 2015;41(9, Part A):10818-27.

42. Venkatesan J, Lowe B, Manivasagan P, Kang K-H, Chalisserry EP, Anil S, et al. Isolation and characterization of nano-hydroxyapatite from salmon fish bone. Materials. 2015;8(8):5426-39.
43. Sun R-X, Lv Y, Niu Y-R, Zhao X-H, Cao D-S, Tang J, et al. Physicochemical and biological properties of bovine-derived porous hydroxyapatite/collagen composite and its hydroxyapatite powders. Ceramics International. 2017;43(18):16792-8.
44. Londoño-Restrepo SM, Ramirez-Gutierrez CF, del Real A, Rubio-Rosas E, Rodriguez-García ME. Study of bovine hydroxyapatite obtained by calcination at low heating rates and cooled in furnace air. Journal of Materials Science. 2016;51(9):4431-41.
45. Oladele IO, Agbabiaka OG, Olasunkanmi OG, Balogun AO, Popoola MO. Non-synthetic sources for the development of hydroxyapatite. J Appl Biotechnol Bioeng. 2018;5(2):88-95.
46. Kabilan N, Babu KD, Karthikeyan N, Chinnakali K. Optical nonlinear properties of hydroxyapatite based materials. Optik. 2022;265:169562.
47. Jaber HL, Hammood AS, Parvin N. Synthesis and characterization of hydroxyapatite powder from natural Camelus bone. Journal of the Australian Ceramic Society. 2018;54(1):1-10.
48. Doostmohammadi A, Monshi A, Fathi MH, Braissant O. A comparative physico-chemical study of bioactive glass and bone-derived hydroxyapatite. Ceramics International. 2011;37(5):1601-7.
49. Ofudje EA, Rajendran A, Adeogun AI, Idowu MA, Kareem SO, Pattanayak DK. Synthesis of organic derived hydroxyapatite scaffold from pig bone waste for tissue engineering applications. Advanced Powder Technology. 2018;29(1):1-8.
50. López EO, Bernardo PL, Checca NR, Rossi AL, Mello A, Ellis DE, et al. Hydroxyapatite and lead-substituted hydroxyapatite near-surface structures: Novel modelling of photoemission lines from X-ray photoelectron spectra. Applied Surface Science. 2022;571:151310.
51. Panda NN, Pramanik K, Sukla LB. Extraction and characterization of biocompatible hydroxyapatite from fresh water fish scales for tissue engineering scaffold. Bioprocess and Biosystems Engineering. 2014;37(3):433-40.
52. DileepKumar VG, Sridhar MS, Aramwit P, Krut'ko VK, Musskaya ON, Glazov IE, et al. A review on the synthesis and properties of hydroxyapatite for biomedical applications. Journal of Biomaterials Science, Polymer Edition. 2022;33(2):229-61.
53. Sunil BR, Jagannatham M. Producing hydroxyapatite from fish bones by heat treatment. Materials Letters. 2016;185:411-4.
54. Hidouri M, Dorozhkin SV, Albeladi N. Thermal behavior, sintering and mechanical characterization of multiple ion-substituted hydroxyapatite

bioceramics. Journal of Inorganic and Organometallic Polymers and Materials. 2019;29:87-100.
55. Neelakandeswari N, Sangami G, Dharmaraj N. Preparation and characterization of nanostructured hydroxyapatite using a biomaterial. Synthesis and Reactivity in Inorganic, Metal-Organic, and Nano-Metal Chemistry. 2011;41(5):513-6.
56. Dorozhkin SV. A history of calcium orthophosphates (CaPO4) and their biomedical applications. Morphologie. 2017;101(334):143-53.
57. Bano N, Jikan SS, Basri H, Bakar SAA, Nuhu AH. Natural hydroxyapatite extracted from bovine bone. Journal of Science and Technology. 2017;9(2).
58. Hussin MSF, Abdulah HZ, Idris MI, Wahap MAA. Extraction of natural hydroxyapatite for biomedical applications—A review. Heliyon. 2022:e10356.
59. Akram M, Ahmed R, Shakir I, Ibrahim WAW, Hussain R. Extracting hydroxyapatite and its precursors from natural resources. Journal of Materials Science. 2014;49(4):1461-75.
60. Sihn Y, Yang H-M, Park CW, Yoon I-h, Kim I. Cation-exchanged hydroxyapatite for strontium separation from groundwater. 2021.
61. Herliansyah MK, Nasution DA, Bin Abdul Shukor MH, Ide-Ektessabi A, Wildan MW, Tontowi AE, editors. Preparation and characterization of natural hydroxyapatite: a comparative study of bovine bone hydroxyapatite and hydroxyapatite from calcite2007: Trans Tech Publ.
62. Ayatollahi MR, Yahya MY, Shirazi HA, Hassan SA. Mechanical and tribological properties of hydroxyapatite nanoparticles extracted from natural bovine bone and the bone cement developed by nano-sized bovine hydroxyapatite filler. Ceramics International. 2015;41(9):10818-27.
63. Ruksudjarit A, Pengpat K, Rujijanagul G, Tunkasiri T. Synthesis and characterization of nanocrystalline hydroxyapatite from natural bovine bone. Current applied physics. 2008;8(3-4):270-2.
64. Khurshid Z, Alfarhan MF, Mazher J, Bayan Y, Cooper PR, Dias GJ, et al. Extraction of Hydroxyapatite from Camel Bone for Bone Tissue Engineering Application. Molecules. 2022;27(22):7946.
65. Le Ho KH, Dao VH, Pham XK, Nguyen PA, Phan BV, Doan TT, et al. Physicochemical properties, acute and subchronic toxicity of nano-hydroxyapatite obtained from Lates calcarifer fish bone. Regional Studies in Marine Science. 2022;55:102560.
66. Indra A, Putra AB, Handra N, Fahmi H, Nurzal, Asfarizal, et al. Behavior of sintered body properties of hydroxyapatite ceramics: effect of uniaxial pressure on green body fabrication. Materials Today Sustainability. 2022;17:100100.

67. Indra A, Hadi F, Mulyadi IH, Affi J, Gunawarman. A novel fabrication procedure for producing high strength hydroxyapatite ceramic scaffolds with high porosity. Ceramics International. 2021;47(19):26991-7001.
68. Odusote JK, Danyuo Y, Baruwa AD, Azeez AA. Synthesis and characterization of hydroxyapatite from bovine bone for production of dental implants. Journal of applied biomaterials & functional materials. 2019;17(2):2280800019836829.
69. Taufik S A, Wiweko A, Yudhanto D, Rizki M, Habib P, Dirja BT, et al. Treatment of bone defects with bovine hydroxyapatite xenograft and platelet rich fibrin (PRF) to accelerate bone healing. International Journal of Surgery Case Reports. 2022;97:107370.
70. Azzallou R, Ouerghi O, Geesi MH, Riadi Y, Taleb MA, Mamouni R, et al. Bovine bone-derived natural hydroxyapatite-supported ZnCl2 as a sustainable high efficiency heterogeneous biocatalyst for synthesizing amidoalkyl naphthols. Journal of Physics and Chemistry of Solids. 2022;163:110533.
71. Han K-S, Sathiyaseelan A, Saravanakumar K, Wang M-H. Wound healing efficacy of biocompatible hydroxyapatite from bovine bone waste for bone tissue engineering application. Journal of Environmental Chemical Engineering. 2022;10(1):106888.
72. Pazourková L, Martynková GS, Šupová M. Ca-deficient hydroxyapatite synthesis on the bioapatite bovine bone substrate study. Materials Today: Proceedings. 2022;52:227-31.
73. Londoño-Restrepo SM, Jeronimo-Cruz R, Rubio-Rosas E, Rodriguez-García ME. The effect of cyclic heat treatment on the physicochemical properties of bio hydroxyapatite from bovine bone. Journal of Materials Science: Materials in Medicine. 2018;29:1-15.
74. Pires LA, de Azevedo Silva LJ, Ferrairo BM, Erbereli R, Lovo JFP, Ponce Gomes O, et al. Effects of ZnO/TiO2 nanoparticle and TiO2 nanotube additions to dense polycrystalline hydroxyapatite bioceramic from bovine bones. Dental Materials. 2020;36(2):e38-e46.
75. Surya P, Nithin A, Sundaramanickam A, Sathish M. Synthesis and characterization of nano-hydroxyapatite from Sardinella longiceps fish bone and its effects on human osteoblast bone cells. Journal of the Mechanical Behavior of Biomedical Materials. 2021;119:104501.
76. Hasan MR, Yasin NSM, Mohd MS. Proximate and morphological characteristics of nano hydroxyapatite (Nano HAp) extracted from fishbone. Journal of Sustainability Science and Management. 2020;15(8):9-21.
77. Venkatesan J, Lowe B, Manivasagan P, Kang KH, Chalisserry EP, Anil S, et al. Isolation and Characterization of Nano-Hydroxyapatite from Salmon Fish Bone. Materials (Basel). 2015;8(8):5426-39.

78. Pal A, Paul S, Choudhury AR, Balla VK, Das M, Sinha A. Synthesis of hydroxyapatite from Lates calcarifer fish bone for biomedical applications. Materials Letters. 2017;203:89-92.
79. Shi P, Liu M, Fan F, Yu C, Lu W, Du M. Characterization of natural hydroxyapatite originated from fish bone and its biocompatibility with osteoblasts. Materials Science and Engineering: C. 2018;90:706-12.
80. Ahmad Fara ANK, bin Yahya MA, Abdullah HZ, editors. Preparation and characterization of biological hydroxyapatite (HAp) obtained from Tilapia fish bone2015: Trans Tech Publ.
81. Popescu-Pelin G, Ristoscu C, Duta L, Pasuk I, Stan GE, Stan MS, et al. Fish bone derived bi-phasic calcium phosphate coatings fabricated by pulsed laser deposition for biomedical applications. Marine drugs. 2020;18(12):623.
82. Elango J, Zhang J, Bao B, Palaniyandi K, Wang S, Wenhui W, et al. Rheological, biocompatibility and osteogenesis assessment of fish collagen scaffold for bone tissue engineering. International Journal of Biological Macromolecules. 2016;91:51-9.
83. Pon-On W, Suntornsaratoon P, Charoenphandhu N, Thongbunchoo J, Krishnamra N, Tang IM. Hydroxyapatite from fish scale for potential use as bone scaffold or regenerative material. Materials Science and Engineering: C. 2016;62:183-9.
84. Manalu J, Soegijono B, Indrani D. Characterization of Hydroxyapatite Derived from Bovine Bone. 2015.
85. Sathiyavimal S, Vasantharaj S, LewisOscar F, Selvaraj R, Brindhadevi K, Pugazhendhi A. Natural organic and inorganic–hydroxyapatite biopolymer composite for biomedical applications. Progress in Organic Coatings. 2020;147:105858.
86. Ribeiro N, Sousa A, Cunha-Reis C, Oliveira AL, Granja PL, Monteiro FJ, et al. New prospects in skin regeneration and repair using nanophased hydroxyapatite embedded in collagen nanofibers. Nanomedicine: Nanotechnology, Biology and Medicine. 2021;33:102353.
87. Bano N, Abu Bakar SAS, Jikan SS, Basri H, Kanasan N. Extraction of biological apatite from cow bone at different calcination temperatures: a comparative study. Key Engineering Materials. 2019;796:46-52.
88. Mondal S, Mondal B, Dey A, Mukhopadhyay S. Studies on Processing and Characterization of Hydroxyapatite Biomaterials from Different Bio Wastes. Journal of Minerals and Materials Characterization and Engineering. 2012;11:55-67.
89. Zhang L, Zhang C, Zhang R, Jiang D, Zhu Q, Wang S. Extraction and characterization of HA/β-TCP biphasic calcium phosphate from marine fish. Materials Letters. 2019;236:680-2.

90. Balamurugan A, Rebelo AHS, Lemos AF, Rocha JHG, Ventura JMG, Ferreira JMF. Suitability evaluation of sol–gel derived Si-substituted hydroxyapatite for dental and maxillofacial applications through in vitro osteoblasts response. Dental Materials. 2008;24(10):1374-80.
91. Walsh PJ, Buchanan FJ, Dring M, Maggs C, Bell S, Walker GM. Low-pressure synthesis and characterisation of hydroxyapatite derived from mineralise red algae. Chemical Engineering Journal. 2008;137(1):173-9.
92. Monballiu A, Desmidt E, Ghyselbrecht K, Meesschaert B. Phosphate recovery as hydroxyapatite from nitrified UASB effluent at neutral pH in a CSTR. Journal of Environmental Chemical Engineering. 2018;6(4):4413-22.
93. Govindaraj D, Rajan M. Synthesis and Spectral Characterization of Novel nano-Hydroxyapatite from Moringaoleifera Leaves. Materials Today: Proceedings. 2016;3(6):2394-8.
94. Salma-Ancane K, Stipniece L, Irbe Z. Effect of biogenic and synthetic starting materials on the structure of hydroxyapatite bioceramics. Ceramics International. 2016;42(8):9504-10.
95. Deng K, Chen H, Dou W, Cai Q, Wang X, Wang S, et al. Preparation and characterization of porous HA/β-TCP biphasic calcium phosphate derived from butterfish bone. Materials Technology. 2022;37(10):1388-95.
96. Huang Y-C, Hsiao P-C, Chai H-J. Hydroxyapatite extracted from fish scale: Effects on MG63 osteoblast-like cells. Ceramics International. 2011;37(6):1825-31.
97. Shaltout AA, Allam MA, Moharram MA. FTIR spectroscopic, thermal and XRD characterization of hydroxyapatite from new natural sources. Spectrochimica Acta Part A: Molecular and Biomolecular Spectroscopy. 2011;83(1):56-60.
98. Rabiei M, Palevicius A, Monshi A, Nasiri S, Vilkauskas A, Janusas G. Comparing methods for calculating nano crystal size of natural hydroxyapatite using X-ray diffraction. Nanomaterials. 2020;10(9):1627.
99. Plumbum I. Synthesis and characterization of hydroxyapatite from bulk seashells and its potential usage as lead ions adsorbent. Malaysian Journal of Analytical Sciences. 2017;21(3):571-84.
100. Vallet-Regí M, González-Calbet JM. Calcium phosphates as substitution of bone tissues. Progress in Solid State Chemistry. 2004;32(1):1-31.
101. Klinkaewnarong J, Utara S. Ultrasonic-assisted conversion of limestone into needle-like hydroxyapatite nanoparticles. Ultrasonics Sonochemistry. 2018;46:18-25.
102. Wu S-C, Tsou H-K, Hsu H-C, Hsu S-K, Liou S-P, Ho W-F. A hydrothermal synthesis of eggshell and fruit waste extract to produce nanosized hydroxyapatite. Ceramics International. 2013;39(7):8183-8.

103. Ofudje EA, Adedapo AE, Oladeji OB, Sodiya EF, Ibadin FH, Zhang D. Nano-rod hydroxyapatite for the uptake of nickel ions: Effect of sintering behaviour on adsorption parameters. Journal of Environmental Chemical Engineering. 2021;9(5):105931.
104. Sharma C, Dinda AK, Potdar PD, Chou C-F, Mishra NC. Fabrication and characterization of novel nano-biocomposite scaffold of chitosan–gelatin–alginate–hydroxyapatite for bone tissue engineering. Materials Science and Engineering: C. 2016;64:416-27.
105. Bayar N, Kriaa M, Kammoun R. Extraction and characterization of three polysaccharides extracted from Opuntia ficus indica cladodes. International Journal of Biological Macromolecules. 2016;92:441-50.
106. Aarthy S, Thenmuhil D, Dharunya G, Manohar P. Exploring the effect of sintering temperature on naturally derived hydroxyapatite for bio-medical applications. Journal of Materials Science: Materials in Medicine. 2019;30:1-11.
107. Jindapon N, Klinmalai P, Surayot U, Tanadchangsaeng N, Pichaiaukrit W, Phimolsiripol Y, et al. Preparation, Characterization, and Biological Properties of Hydroxyapatite from Bigeye Snapper (Priancanthus tayenus) Bone. International Journal of Molecular Sciences. 2023;24(3):2776.
108. Grassino AN, Brnčić M, Vikić-Topić D, Roca S, Dent M, Brnčić SR. Ultrasound assisted extraction and characterization of pectin from tomato waste. Food chemistry. 2016;198:93-100.
109. Alici EH, Bilgicli AT, Tuezuen B, Günsel A, Arabaci G, Yarasir MN. Alkyl chain modified metalophthalocyanines with enhanced antioxidant-antimicrobial properties by doping Ag+ and Pd2+ ions. Journal of Molecular Structure. 2022;1257:132634.
110. Akindoyo JO, Beg MDH, Ghazali S, Akindoyo EO, Jeyaratnam N, editors. Synthesis of hydroxyapatite through ultrasound and calcination techniques2017: IOP Publishing.
111. Kokubo T, Yamaguchi S. Simulated body fluid and the novel bioactive materials derived from it. Journal of Biomedical Materials Research Part A. 2019;107(5):968-77.
112. Epp J. X-ray diffraction (XRD) techniques for materials characterization. Materials characterization using nondestructive evaluation (NDE) methods: Elsevier; 2016. p. 81-124.
113. Nilen R, Richter P. The thermal stability of hydroxyapatite in biphasic calcium phosphate ceramics. Journal of Materials Science: Materials in Medicine. 2008;19(4):1693-702.
114. Latif AFA, Mohd Pu'ad NAS, Ramli NAA, Muhamad MS, Abdullah HZ, Idris MI, et al., editors. Extraction of biological hydroxyapatite from tuna fish bone for biomedical applications2020: Trans Tech Publ.

115. Pu'ad NASM, Haq RHA, Noh HM, Abdullah HZ, Idris MI, Lee TC. Nano-size hydroxyapatite extracted from tilapia scale using alkaline heat treatment method. Materials Today: Proceedings. 2020;29:218-22.
116. Ahamed AF, Manimohan M, Kalaivasan N. Fabrication of biologically active fish bone derived hydroxyapatite and montmorillonite blended sodium alginate composite for in-vitro drug delivery studies. Journal of Inorganic and Organometallic Polymers and Materials. 2022;32(10):3902-22.
117. Diaz-Rodriguez P, Landin M. Biomorphic ceramics for drug delivery in bone tissue regeneration. Current Pharmaceutical Design. 2017;23(24):3507-14.
118. Murugapandian R, Clement S, Uthirapathy V. Fabrication and In Vitro Drug Delivery Evaluation of Cephalexin Monohydrate-Loaded PLA: PVA/HAP: TiO2 Fibrous Scaffolds for Bone Regeneration. ACS Omega. 2023.
119. Wang Y, Feng T, Xia Q, Zhou C, Cao J. The influence of comminuting methods on the structure, morphology and calcium release of chicken bones. Frontiers in Nutrition. 2022:989.
120. Alshemary AZ, Akram M, Taha A, Tezcaner A, Evis Z, Hussain R. Physico-chemical and biological properties of hydroxyapatite extracted from chicken beaks. Materials Letters. 2018;215:169-72.

الخلاصة

يُفضل هيدروكسيباتيت (HAp) بانتظام على المواد الحيوية الأخرى التي تحتوي على فوسفات الكالسيوم في العمليات الجراحية لتقويم العظام نظرًا لقدرته على إعادة امتصاصه تحت المواقف الفسيولوجية , هيدروكسيباتيت (HAp) مادة حيوية يمكن استخلاصها من المصادر الطبيعية, تم استخدام HAp على نطاق واسع في البرامج الطبية الحيوية نظرًا للنشاط الحيوي الرائع والتوافق الحيوي المفرط والتوصيل العظمي الجيد للغاية. تتكون الرسالة من ثلاثة فصول ، الفصل الأول هو مقدمة عن كيفية استخراج هيدروكسيباتيت العضوي من الموارد الطبيعية لفائدة الطب الحيوي , يصف الفصل الثاني الجزء العملي الذي يتضمن معالجة العينات واستخراج هيدروكسيباتيت ، ويشرح الفصل الأخير النتائج ومناقشة النتائج , في هذا البحث مجموعة من الهيدروكسيباتيت (HAp) المستخرج من مدينة ميسان في العراق من الموارد الطبيعية للعظام وهي تتكون من عظام السمك وعظام الخروف وعظام الأغنام من خلال استخدام طريقة التكليس الحراري في درجات حرارة مختلفة , تم التشخيص الذي يتم إجراؤه من خلال حيود الأشعة السينية (XRD) ، والفحص المجهري الإلكتروني لمسح الانبعاث (FESEM) المرتبط بتحليل الأشعة السينية المشتتة للطاقة (EDX) ، واستراتيجيات مقياس الطيف الضوئي بالأشعة تحت الحمراء (FTIR)لتقييم تكوين الطور ، ومورفولوجيا السطح والتركيبات الكيميائية لهيدروكسيباتيت .(HAp) تم تغيير سلوك الذوبان في المختبر لجميع هيدروكسيباتيت إلى تقييم عن طريق غمر العينات في سائل الخلية العظمية الافتراضية (SBF) على مدار 14 يومًا عند 37 درجة مئوية. وتمت دراسة الفعالية البايلوجية ومضادات البكتريا باستخدام هيدروكسيباتيت (HAp) نوعين من البكتريا، وتؤيد أن هيدروكسيباتيت (HAp) يمكن تطويره بالإضافة إلى خصائص تحرير العظام المضادة للبكتيريا من المضادات الحيوية. أن هيدروكسيباتيت المحضر يمكن أن يكون أيضًا بمثابة هياكل إطلاق دواء مُدارة ، فقد تم تضمين أموكسيسيلين وتتراسيكلين وسيفاليكسين في هيدروكسيباتيت وأكدت النتائج إطلاقها إطلاقًا مناسبًا للدواء على مدى 7 أيام محملة HAp من عظام السمك , تم اكتشاف الإطلاق التراكمي بنسبة 75% و 79% و 95% للأموكسيسيلين والتتراسيكلين والسيفاليكسين على التوالي , بينما من الدجاج 75% و 86% و 96.3 % على التوالي , مع HAp من عظم الغنم 68% و 78% و 75% على التوالي .

جمهورية العراق
وزارة التعليم العالي والبحث العلمي
جامعة ميسان
كلية العلوم
قسم الكيمياء

تحضير و تشخيص هيدروكسي أبيتايت البيولوجي من مصادر طبيعية لبعض التطبيقات الطبية

رسالة مقدمة الى

كلية العلوم / جامعة ميسان جزء من متطلبات نيل شهادة الماجستير في علوم الكيمياء

من الطالبة

دعاء عبود جلوب الموسوي

بكالوريوس علوم كيمياء / جامعة ميسان (2014)

بإشراف

الأستاذ المساعد الدكتور علي طه صالح

2023